Vol. 2. Issue 1, 2016 ISSN: 2453-7314

Central European Researchers Journal

ZILINSKÁ UNIVERZITA UNIVERSITAS SOLNENSIS

CERES

A Word of Welcome from the Editors

Dear Colleagues, Readers and Authors,

We are glad to present next number of the "Central European Researchers Journal (CERES)". Topics of this number cover different investigation in computer science. And we hope that it allows to us to present results of many young researchers, because this journal is platform for publications of PhD students and young researchers first of all. All accepted papers have been reviewed and selected by members of journal's Editorial Board. We hope that these papers will be interesting for readers and these publications will be useful for authors to continue their investigations.

With best wishes

Prof. Vyacheslav Kharchenko
Prof. Elena Zaitseva

Central European Researchers Journal. Volume 2. Issue 1
Editor-in-chief: Kharchenko Vyacheslav, Zaitseva Elena

Addres of the editorial office: Central European Researchers Journal - editorial, Faculty of Management Science and Informatics, University of Zilina, Univerzinta 8215/1, 01026, Zilina, Slovakia, editorial@ceres-journal.eu
Each paper was reviewed by reviewers.
Publisher: JMTM, s.r.o., Sad SNP 8, 010 01, Zilina, Slovakia, publisher@jmtm.sk
Published biannually
ISSN: 2453-7314
June 2016

Contents

Modelling Dental X-ray Examinations for Assessment of Radiation Doses to Patients

Kristina O. Makarevich, Victor F. Minenko, Semen A. Kutsen

***Abstract*—**The work is connected with modelling dental radiographic examinations for evaluating absorbed and effective doses to patients. The X-ray set model with the source of radiation and the models of irradiated objects (the reference voxel phantoms of an adult male and female) were constructed. Monte Carlo simulation of X-rays transport in the patient body during dental radiography was performed. Radiation doses to organs and tissues and effective doses for different types of dental examinations and features of X-ray tube were obtained.

***Keywords*—** Dental radiography, Monte Carlo method, radiation doses, voxel phantoms, X-ray tube.

I. Introduction

Currently X-ray examinations became the leading and widely used method in identifying many dental system diseases. The tendency of fast dental radiology development causes to treat with special attention to observance of radiation safety during dental examinations. For example, medical exposure is the second most important source of irradiation after natural sources for the population of Belarus. Meanwhile its contribution to the radiation exposure of the population is almost entirely formed by diagnostic and preventive medical examinations embracing all age groups [1].

In this context the problem of determining the radiation burden to patients from medical X-ray examinations becomes of current interest. And there exist a very convenient tool for comparing different exposure methods and procedures. It's the effective dose proposed by the International Commission on Radiological Protection (ICRP) at a modified interpretation [2].

In practice radiologists receive the effective dose to a patient using special tables that in very common form take into account the impact on dose from X-ray unit model, procedure type and X-ray field dimensions. But in recent years new types of X-ray sets are widely used in dental practice. They have different workload, various anode voltage and different radiation output. Thus revising these tables, reassessing radiation field distribution and preparing more reliable dose estimations are required. Also all these new data must be received considering exposure séance parameters, radiation output and patient anthropometric characteristics.

As it is rather difficult or in most cases impossible to estimate doses to patient organs and tissues then the only appropriate way of evaluating these doses is modelling the exposure procedure. The simulation allows receiving the distribution of absorbed and equivalent doses in human body, estimating the effective dose for particular examination type and exposure set, or determining desired X-ray set parameters combination.

In this work the Monte Carlo method was applied to simulate the X-ray radiation transport in the environment. Currently method Monte Carlo is widely used for dosimetry of radiological examinations in medicine [3]. There are some computer codes (EGS, MCNP, FLUKA, GEANT, etc.) that implement method Monte Carlo for solving the task of various particles transport in different media [4-7]. These programs require such input data as the X-ray source model and the irradiated object model for calculating doses in the human body.

Thus all work connected with estimating doses to patients from dental X-ray examinations can be divided into several stages:

K. O. Makarevich, Research Institute for Nuclear Problems of Belarusian state University, Minsk, Belarus (e-mail: kristinanevdokh@tut.by).
V. F. Minenko, Research Institute for Nuclear Problems of Belarusian state University, Minsk, Belarus (e-mail: vminenko@list.ru).
S. A. Kutsen, Research Institute for Nuclear Problems of Belarusian state University, Minsk, Belarus (e-mail: kut@inp.bsu.by).

1. Development of a diagnosis dental X-ray set model with a source of radiation;
2. Constructing human body model taking into account the geometry of exposure;
3. Calculation of the absorbed dose distribution in patient's body and determining the effective dose with Monte Carlo method.

In this work the software MCNP (Monte Carlo N-particles Transport Code, Los Alamos National Laboratory, USA) version 4B was used for Monte Carlo modelling.

II. Dental X-ray Set Model

The important element of modelling is obtaining radiation spectrum of X-ray set. Nowadays there are three basic directions of radiation spectrum measuring, modelling and calculating: experimental methods, theoretical methods (Monte Carlo simulation) and semi-empirical methods [8]. Each of these techniques has its advantages and disadvantages, but the Monte Carlo method provides more appropriate results primarily because it uses realistic representation of radiation interaction with matter and detailed description of problem geometry.

Unfortunately, it is difficult to implement the detailed X-ray tube model because of the lack of manufacturer detailed information about tube constituent elements and their material composition. Furthermore, simulating such a model takes much computer time as it takes into account all physical processes included in generation of bremsstrahlung radiation although most of them will not be used for final spectrum. Therefore, the X-ray emitter was modelled by a point source with predetermined energy spectrum in this work.

To obtain the X-ray tube energy spectrum the TASMIP (Tungsten Anode Spectral Model Interpolating Polynomials) model was used. It is considered to be the most appropriate one for modelling typical X-ray examinations using X-ray tube with a tungsten anode that operates in the anode voltage range from 30 to 140 kV [9]. TASMIP model based on polynomial interpolation of experimentally measured emission spectra of X-ray tube with a tungsten anode actually acts as X-ray tube model as it considers spectrum dependence on the anode voltage, ripple and total filtration.

The model of typical X-ray set comprising TASMIP was developed with the help of MCNP and Mathematica. This model does not require simulating the X-ray tube internal structure and operation mode but nevertheless it takes into account:

- anode voltage (V);
- total beam filtration (d);
- beam size;
- distance from radiation source focus to the surface of the irradiated object (FSD);
- anode voltage ripple;
- characteristics of the forming system.

The necessary spectra were obtained by setting definite anode voltage, filter thickness and ripple.

All dental X-ray sets use systems that form the field of irradiation. Usually it is a lead director cone with a round or rectangular diaphragm at the end. 20 cm or 30 cm director cones are often used in modern dental X-ray sets. They form either a round field having a diameter of 6 cm or a rectangular field with dimensions (3-3.5) cm × (4-4.5) cm on a flat surface. In this work simulation was performed for the X-ray set having a tube with director cone length of 20 cm and forming a rectangular field of 3 cm × 4 cm.

III. Model of the irradiated object

As mentioned above the MCNP program requires a computational model of human body (phantom) with detailed description of the internal structure, organs positions, tissues density and composition for calculating the absorbed dose distribution in the human body.

According to the ICRP recommendations one should use the reference voxel adult male and female phantoms for dosimetric calculations [10]. These phantoms correspond to standard anatomical data presented in ICRP Publication 89 [11].

The voxel phantom is a computer model of the human placed in a rectangular parallelepiped and divided into equal-size cells (voxels). Each voxel has a number that attributes it to a particular organ or tissue. Voxels that do not belong to phantoms are filled with air. The reference phantoms contain more than 140 different structures, which consist of 50 types of tissues. It allows achieving maximum conformity to the reference individual not only in organs shape and location but also in chemical composition of organs and tissues. There are more than 14 million voxels in the female voxel phantom. Voxel dimensions are 1.78 mm × 1.78 mm ×4.8 mm. The male phantom contains more than 7 million voxels having a size of 2.14 mm× 2.14 mm × 8 mm.

These reference phantoms were found to be too detailed for modelling dental X-ray examinations. Therefore, the phantoms adjustment to the MCNP code was made, i.e. the part of phantom that was directly within the radiation field and the penumbra region located at a distance of 20 cm from the field edge was included into the irradiated zone (see Fig. 1).

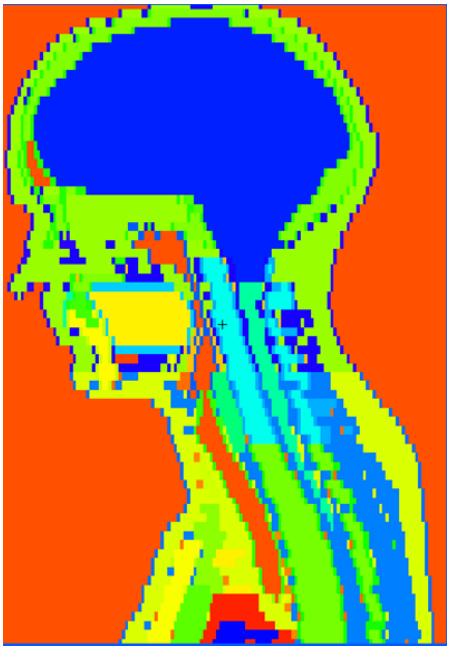

Fig. 1 The phantom part located within the radiation field and the penumbra region

As mandible and maxilla teeth were not distinguished in the voxel phantoms, it was necessary to modify these phantoms by performing separation of the teeth. For this purpose, the images of transverse sections that passed through the bite plane of male and female phantoms were obtained using the MCNP code. Then the jaw curve points array was obtained with the help of GetData software. These points were processed by a specially developed program in Mathematica. This program segregates the teeth of mandible and maxilla using biometric data on the adult patient average teeth size.

IV. Geometry of exposure

For obtaining an undistorted tooth image on an X-ray field it is necessary for radiologists to abide two following techniques for intraoral examinations: the bisecting angle technique (isometric technique) and the tangent technique. Therefore, these two techniques must be taken into consideration during simulation.

Thus, in this work the source position and the central beam direction were chosen in such a way that the central beam could hit perpendicularly the plane dividing the angle between the tooth axis and the radiographic field plane (the isometric technique). Simultaneously, the central beam was directed toward the tangent to the targeted tooth arc (the tangent technique). In this case the upper teeth roots were projected on the Camper plane while the lower teeth roots were projected on the plane located 0.5 cm above the lower jaw edge [12].

In order to apply the tangent technique envelope curves were plotted to each dental arch (for the mandible and the maxilla). Then normal to the middle of certain tooth was drawn (see Fig. 2).

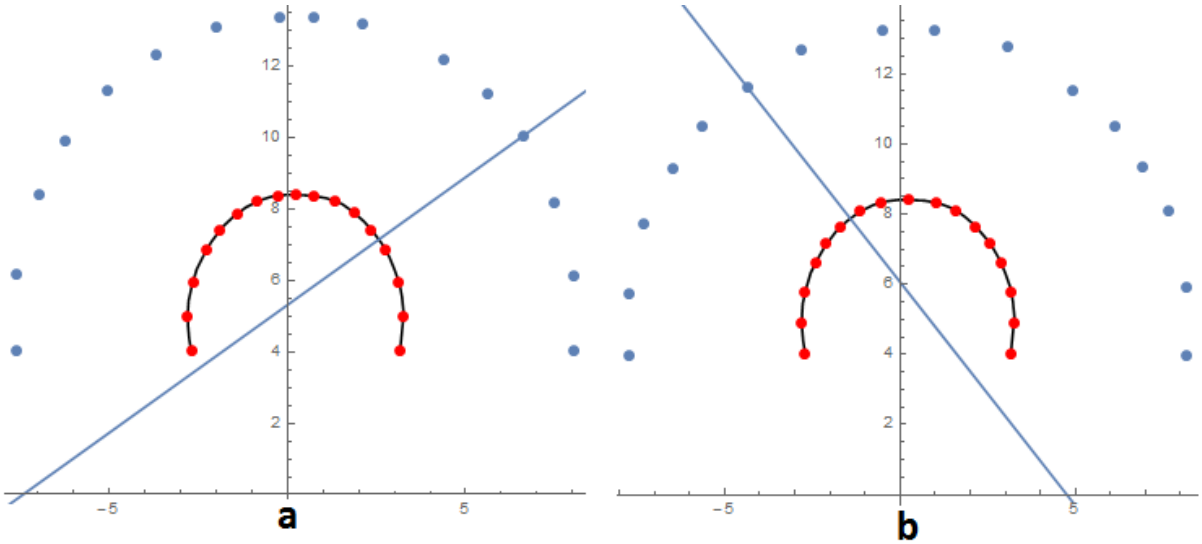

Fig. 2 The tangent technique applications for the mandible teeth (a) and the maxilla teeth (b) of the female phantom

The equations that describe the Camper plane and the corresponding plane for the mandible were derived to apply the isometric technique. The inclination angles of these planes to the horizontal plane were calculated. The direction of the central X-ray beam was chosen so that the beam could be normal to the tangent and form the proper angle (see Table 1) with a certain plane.

TABLE I
Inclination Angles for Intraoral Contact Radiography [12]

Teeth	Maxilla	Mandible
Incisors	+55°…+65°	-20°
Canines	+45°	-15°
Premolars	+35°	-10°
Molars	+25°…+30°	-5°…0°

V. METHODOLOGY OF CALCULATING RADIATION DOSES

Calculating the effective dose and radiation doses to organs and tissues was performed in accordance with the ICRP recommendations [2].

In order to find the absorbed dose to an organ or a tissue, the dose values obtained with the help of MCNP were summed up and averaged over the organ or tissue volume

$$\overline{D}_{T,R} = \frac{\sum_{i=1}^{N} D_{i,T}}{N_T}, \tag{1}$$

where $D_{i,T}$ is the value of the absorbed dose in the *i*th voxel of the organ/tissue *T*; N_T is the number of voxels in the organ/tissue *T*.

The equivalent dose H_T to an organ or a tissue is numerically equal to the average absorbed dose $\overline{D}_{T,R}$ as the weighting factor for X-rays is $w_R = 1$

$$H_T = \sum_R w_R \cdot \overline{D}_{T,R}\,. \tag{2}$$

The effective dose *E* was calculated using average values of sums of equivalent doses to organs and tissues of the reference male and female

$$E = \sum_T w_T \cdot \left[\frac{H_T^M + H_T^F}{2} \right], \tag{3}$$

where w_T is the weighting factor for the organ/tissue *T*; H_T^M is the equivalent dose to the organ/tissue *T* of the reference male; H_T^F is the equivalent dose to the organ/tissue *T* of the reference female.

TABLE II
RECOMMENDED TISSUE WEIGHTING FACTORS [2]

Tissue	w_T	$\sum w_T$
Bone marrow (red), colon, lungs, stomach, breast, remainder tissue	0.12	0.72
Gonads	0.08	0.08
Bladder, esophagus, liver, thyroid	0.04	0.16
Bone surface, brain, salivary glands, skin	0.01	0.04
	Total	1
Remainder tissues: adrenals, extrathoratic region, gall bladder, heart, kidneys, lymphatic nodes, muscle, oral mucosa, pancreas, prostate (only for male), small intestine, spleen, thymus, uterus/cervix (only for female).		

It is worth noting that the equivalent doses to the organs and tissues from the remainder tissues category should be calculated according to [2] as

$$H_{other}^M = \frac{1}{13} \sum_T^{13} H_T^M \tag{4}$$

and

$$H_{other}^F = \frac{1}{13} \sum_T^{13} H_T^F \tag{5}$$

where *T* is a remainder tissue from Table 2.

As MCNP gives all simulation results per one emitted particle it is necessary to multiply the result by the number of emitted gamma-quanta to obtain real values of doses. As a result, the average radiation dose to the organ/tissue T ($\overline{D}_T$) is determined by the expression

$$\overline{D}_T = 2\pi \cdot \left(1 - \cos\left(\frac{\theta}{2}\right)\right) \cdot R^2 \cdot \left[\frac{R_0}{R}\right]^2 \cdot N_\gamma \cdot \overline{D}_{T,R}, \frac{Gy}{mA \cdot s} \tag{6}$$

where $\overline{D}_{T,R}$ is the average value of the absorbed dose obtained by MCNP, $\left(\frac{Gy}{photon}\right)$; $N_\gamma = \int \Phi^*(E,d,V,\zeta)\,dE$ is the flux of gamma-quanta produced by TASMIP at a given distance R , voltage V, filtration d and ripple ζ and normalized to 1 A, $\left(\frac{photon}{mA \cdot s \cdot mm^2}\right)$; $\Phi^*(E,d,V,\zeta)$ is the interpolated function of the TASMIP source, $\left(\frac{photon}{mA \cdot s \cdot mm^2 \cdot keV}\right)$; $R_0 = 100cm = 1000mm$ is the distance at which TASMIP spectra are given; R is the distance between the source and the irradiated surface, (mm); θ is the angle of the cone with the vertex at the focus and circumscribed around the field of radiation, (°); $2\pi \cdot \left(1 - \cos\left(\frac{\theta}{2}\right)\right) \cdot R^2$ is the surface area of the cone base at the distance R from its vertex, (mm^2).

In expression (6) the correction factor η should be introduced for a rectangular field with dimensions of a and b:

$$\eta = \frac{4 \cdot a \cdot b}{\pi \cdot (a^2 + b^2)}. \tag{7}$$

The result of calculating doses according to (6) is given per 1 mA and thus it cannot be used for estimating the effective dose from a particular X-ray set as this value does not include the specific characteristics of this set. Therefore, for calculating the effective dose E the following expression is used in practice [13]:

$$E = R \cdot I \cdot t \cdot K_e, \tag{8}$$

where R is the radiation output of the X-ray tube, $\left(\frac{mGy \cdot m^2}{mA \cdot s}\right)$; I is the X-ray tube current, (mA); t is the exposure time, (s); K_e is the conversion coefficient from the radiation output of the X-ray tube to the effective dose, $\left(\frac{\mu Sv}{mGy \cdot m^2}\right)$. The coefficient K_e takes into account a type of X-ray examination, the irradiation projections, field size, focus distance and anode voltage of the X-ray tube. This conversion coefficient is determined dividing the effective dose value by the radiation output.

The radiation output of the X-ray set is calculated by means of the absorbed dose (or air kerma) multiplying by a squared distance of 1 m and dividing by the exposure setting 1 mA·s. This absorbed dose (or air kerma) is measured in free air on the primary X-rays beam axis at a distance of 1 m from the X-ray tube focus for a given anode voltage [13].

The radiation output for the TASMIP spectrum can be obtained using the following formula

$$R_{TASMIP}(d,V,\zeta) = \frac{R_0^2}{R^2} \int_{E_1}^{E_2} \Phi^*(E,d,V,\zeta) \cdot F(E) \cdot dE \tag{9}$$

where $F(E)$ is the function that converts the flux to the kerma [13].

VI. Results and discussion

Dose distributions in a patient's body, doses to certain organs and tissues of male and female adult phantoms were obtained. The effective doses for different procedures of contact intraoral radiography were calculated.

The conversion coefficients calculated for three values of high voltage (60 kV, 65 kV and 70 kV) for a rectangular field of 3 cm × 4 cm are shown in Table 3. They represent well the effective dose dependence on the tube angle inclination but much less on anode voltage. For this reason the conversion coefficients proposed in different methodical documents should be divided into a larger number of gradations depending on the X-ray tube inclination angle.

TABLE III
THE CONVERSION COEFFICIENTS FOR DIFFERENT EXAMINATIONS OF MAXILLA

Parameters			Examinations			
V, kV	d_{Al}, mm	R, $\mu Gy \cdot m^2 / mA \cdot s$	Incisors	Canines	Premolars	Molars
60	3	0.028	29.5	27.3	14.7	14.
65	3	0.035	30.9	28.5	15.9	15.5
70	3	0.043	32.2	29.6	17.2	16.6

Table 4 shows the average effective doses to the male and female phantoms organs and tissues for contact intraoral radiography of the maxilla teeth for anode voltage of 60 kV. The calculations were performed for such typical parameters of dental radiography as FSD=20 cm, total aluminium filtration d_{Al}=3 mm, rectangular field of 3 cm × 4 cm, exposure setting 1 mA·s.

TABLE IV
DOSES TO ORGANS AND TISSUES FOR CONTACT RADIOGRAPHY OF MAXILLA TEETH

Organs and tissues	Examinations			
	Incisors	Canines	Premolars	Molars
Extrathoratic region, μSv	51.5	45.8	12.4	10.1
Oral mucosa, μSv	21.0	21.6	14.6	9.6
Bone surface, μSv	4.5	4.4	4.3	5.1
Salivary glands, μSv	1.5	1.7	2.2	5.9
Red bone marrow, μSv	0.6	0.5	0.6	0.7
Skin, μSv	0.5	0.4	0.4	0.4
Brain, μSv	0.4	0.3	0.5	0.7
Thyroid, μSv	0.2	0.2	0.2	0.1
Effective dose, μSv	0.9	0.8	0.4	0.4

Red bone marrow, skin and thyroid are irradiated in least. Wherein, doses to them are practically independent of the tube inclination angle. However, the effective dose increases linearly with increase of high tube voltage.

VII. Conclusion

Modelling different dental exposure procedures for assessment of absorbed and effective doses was presented in this work. The X-ray set model forming a rectangular field of 3 cm × 4 cm at a distance of 20 cm from the tube focus was created. The TASMIP model was used for simulating X-ray spectra. Doses estimation was performed based on the Monte Carlo method with the help of the MCNP. The results can be used for preparing methodical documents regarding doses assessment for different dental examinations and for various X-ray tube

characteristics. They also can be used for developing optimal irradiation procedures.

In the future we plan to evaluate effective doses to children and adolescents during dental X-ray examinations.

References

[1] G. V. Chizh, "Actual problems of radiation diagnosis, radiotherapy and radiation safety: materials of the international scientific-practical conference," Minsk, 2008, pp. 180–183. (in Russian)

[2] International Commission on Radiological Protection, *The 2007 Recommendations of the Commission on Radiological Protection. ICRP Publication 103*, *Ann. ICRP 37 (2-4).* Pergamon Press, 2007, 332 p.

[3] M. R. Ay, M. Shahriari, S. Sarkar, M. Adib, H. Zaidi, "Monte Carlo simulation of X-ray spectra in diagnosis radiology and mammography using MCNP4C", *Phys. Med. Biol.*, vol. 49, no. 21, Oct. 2004, pp. 4897.

[4] I. Kawrakov, D. Rogers, "The EGSnrc code system: Monte Carlo simulation of electron and photon transport". PIRS-701. NRCC. Ottawa, 2000.

[5] J. F. Briesmeister, *et al*, "MCNP-A General Monte Carlo N-Particle Transport Code, Version 4B,"NM: Los Alamos National Laboratory, 1997. 736 p.

[6] A. Fasso, A. Ferrari, P. R. Sala, "Electron-photon transport in FLUKLA: status," Advanced Monte Carlo for radiation physics, particle transport simulation, and applications: proceedings of the Monte Carlo 2000 Conference, Lisbon, 32–26 October 2000. Springer Berlin Heidelberg, 2001, pp. 159-164.

[7] Geant Collaboration, "Geant-4 User's Guide for Application Developers", 2005, 350 p.

[8] B. R. Lankipalli, W. D. McDavid, S. B. Dove, E. Wieckowa, R. G. Waggener, J. R. Mercier, "Comparison of five methods for the derivation of spectra for a constant potential dental X-ray unit," *Dento-Maxillo-Facial Radiology*, vol. 30, no. 5, 2001, pp. 264-269.

[9] J. M. Boone, J. A. Seibert, "An accurate method for computer-generating tungsten anode x-ray spectra from 30 to 140 keV," *Med. Phys*, vol. 24, no. 1, 1997, pp. 1661-1670.

[10] International Commission on Radiological Protection, *Adult Reference Computational Phantoms. ICRP Publication 110*, *Ann. ICRP.* Pergamon Press, 2009, 165 p.

[11] International Commission on Radiological Protection, *Basic Anatomical and Physiological Data for Use in Radiological Protection Reference Values*. ICRP Publication 89. Pergamon Press, 2003, 265 p.

[12] A.Y.Vasiliev, Y. I. Vorobiev, V. P. Truten "Radiation diagnostics in dentistry," M.:Medika, 2007, 496 p. (in Russian)

[13] Guidelines 2.6.1.2944-11. "Control of effective doses to patients during medical X-ray examinations," 2001. (in Russian)

Importance of Cyclicality in the Processes of Economic System Development

Katerina O. Udachina, Liliya M. Bandorina

Abstract **–** The cyclical theory has been analyzed in the article. Works of local and foreign scientists has been reviewed. It has been proved that the theory of economic cycles play an important role for entrepreneurs in explaining economic processes and accepting practical solutions for effective development. Factors influencing on the economic behavior of the object in dynamics have been considered, the relationship between economic cycles and object behavior has been investigated, a notion of cyclicality has been defined in a new way.

Keywords **–** cyclicality, dynamics, economic behavior of the object, trend.

I. Introduction

Economic system is constantly evolving due to the influence of endogenous and exogenous factors. The globalization of the economy, accelerate the development of economic, financial, marketing processes, presence of stochastic and dynamic in the economic behavior of the objects exacerbates the problem of the modern economic instability.

The peculiarity of economic conjuncture is very complex and variable combination of component. Structure of the economic signal is divided into "coarse" and "subtle" components. There can be defined trend, seasonality, cyclicality, stochastic "noise" and event-trigger component of dynamics in the general structure. Reasons, changes and forms of dependence of trend and seasonality can be predicted beforehand, that's why their behavior is smooth. They have found ways of detection, selection, presentation, explanation, visualization and application long time ago. Cyclicality [1], stochasticity and event-trigger components are difficult to be predicted because reasons of "subtle" component are not clear; events are difficult to be planned [2]. Economic events are uneven and conflicting and characterized by cyclic processes, which are difficult to be calculated mathematically.

II. Retrospective Of Researches And Publications

Works of the following local and foreign scientists are theoretical and methodological basis of research: V. P. Alexandrova, U. M. Bagal, S. Glazyev, V. Inozemtsev, M. Kondratiev, V. Kotysko, V. Kushlin, K. Marx, V. P. Seminozhenko, M. I. Tugan-Baranovsky, U. V. Yakovets. There are contradictions on the causes of cyclical fluctuations among scientists. Some theoretical foundations and practical results don't reflect the relationship between cyclicality and economic behavior of the object in full. There is a need to clarify the concept of "cyclicality" and to identify factors influencing the economic behavior of the object in the dynamics that lead to it.

III. Main Part Of Researches

Based on the fact that the structure of the economic process is an free combination of five components, which form together a time series. Its graphically economic conjuncture can be presented in the following way (Fig. 1):

E.A. Udachina - National Metallurgical Academy of Ukraine, Dnepropetrovsk, Ukraine (e-mail: eudachina7@yandex.ru).
L.N. Bandorina - National Metallurgical Academy of Ukraine, Dnepropetrovsk, Ukraine (e-mail: bandorina1@yandex.ru).

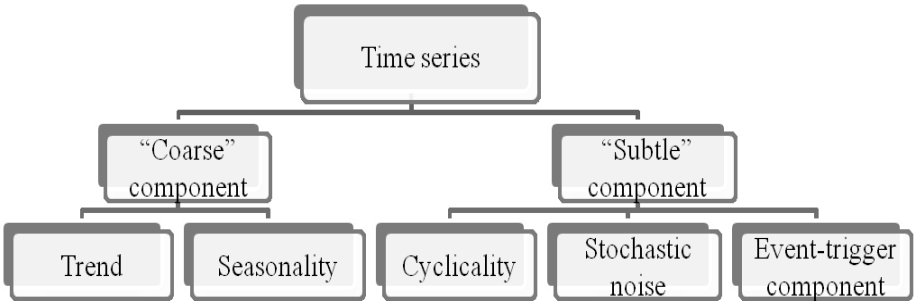

Fig. 1 - Structure of time series of economic process [2]

Many scientists studied time series, including V. A. Bessonov [3], who defined time series as an ordered set that characterizes changes of index in time.

Concept of development tendency does not have enough clear definition. In statistical literature a tendency of development is understood as the long-term evolution, that is tried to be imagined in trajectory. It is assumed that this trajectory describes the basic movement regularity over time and at some extent it is free from random effects and called the trend The trend describes actual generalized tendency of processes over time [4].

As tendencies of changes of time series indicators are very different, then the trends may have different forms, which are often represented as a models of trends that are based on functions (Table I).

TABLE I –
FUNCTIONS OF TRENDS MODELS

Name of function	Function
Linear function	$Y(x) = a_0 + a_1 \times x$
Square function	$Y(x) = a_0 + a_1 \times x + a_2 \times x^2$
Power function	$Y(x) = a_0 + a_1 \times x_2^a$
Polynomial functio	$Y(x) = a_0 + a_1 \times x + a_2 \times x^2 + \ldots + a_n \times t^n$
Logarithm function	$Y(x) = a_0 + a_1 \times x \times \log(x)$
Exponential function	$Y(x) = a_0 + a_1 \times b^x$
Logistic functions: P. Reed's function Gompertz's function	$Y(x) = \frac{a}{1 + b \times e^{-c \times x}}$; $Y(x) = \frac{(Y_{\max} - Y_{\min})}{1 + e^{a_0 + a_1 \times x}} + Y_{\min}$ $Y(x) = k \times a^{b \times x}$

As for the element of time series such as seasonality, modern scientists understand this concept as a stable over time periodicity of economic phenomena development and they use the term "season" for predicting any systematic fluctuations. Factor of seasonality cannot be displayed according to data of whole year or average annual data. Time series can be used for investigating the influence of seasonality. These time series contain information about the value of the index per quarters, months, weeks, days or hours [5].

V. A. Bessonov [3] divided seasonal component of time series in a cyclic and periodic components. He interpreted cyclicality as repetition of phenomena in general characteristics and also he interpreted periodicity as a special case of cyclicality when the picture is repeated

in detail in each following cycle. He considered seasonal fluctuations as example of cyclicality, because despite on repetition of phenomena in general characteristics, they very often demonstrate changes over time as size and form. In the study of economic dynamics problems in individual phases of the economic cycle the scientist accented that the information can be presented in the form of interval and momental time series [3].

The term of cyclicality is associated with fluctuations of age trends, because it is multi-structural pattern of economic development. Periodic manifestations of various reactions of the economic system by external and internal factors in the dynamics of constantly require scientists to investigate and analyze the causes and consequences of the manifestations of these reactions.

The English scientist W. Jevons the first time tried to investigate the long-term fluctuations in the economy. By analyzing ranks of prices, he noticed repetition of long periods of rising and falling, but could not find an explanation for this phenomenon [6].

Financial and economic dictionary [7] interprets the term of cyclicity in the following way: "the general shape of global economic development and the development of the national economy from one macroeconomic balance to another. This reflects unevenness of various elements of the national economy, change of evolutionary and revolutionary stages of development".

The explanatory dictionary by S. Ozhegov explains term of cycle as a set of events and processes that is circulation over time [8].

Based on the fact that economic changes that are manifested from one state of economy to another one, are repeated periodically, there are four phases of the cycle development. Karl Marx was one of the first economists, who identified four phases in the cycle (Fig. 2).

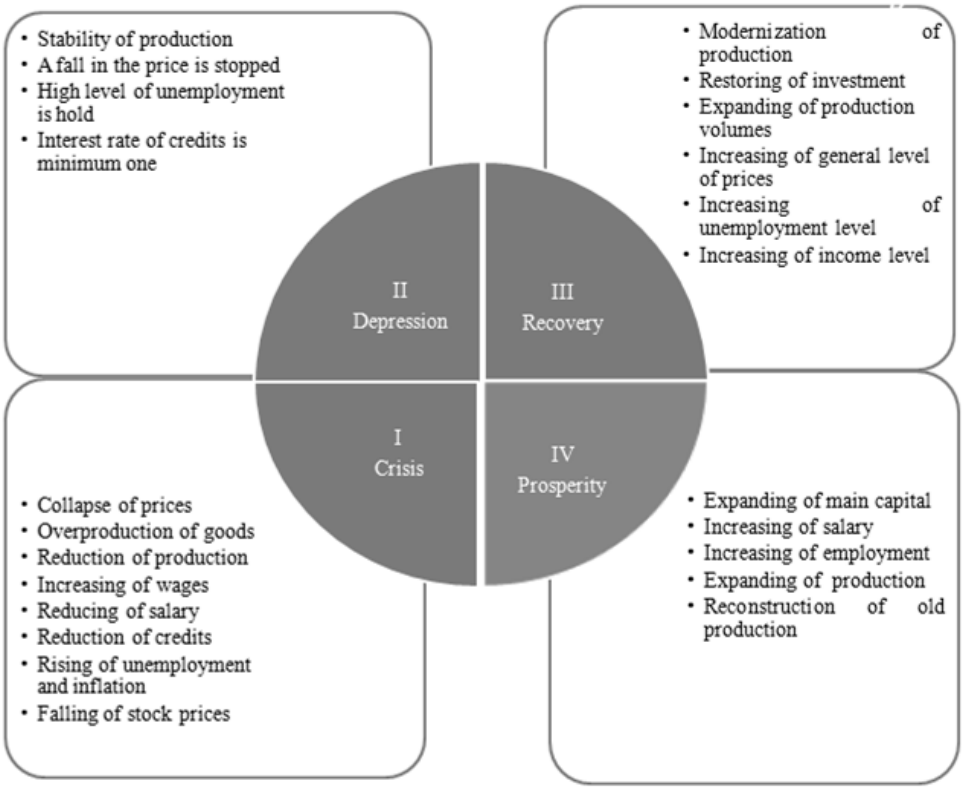

Fig. 2 - Phases of cyclical development

Graphically dynamic of indicator of economic behavior can submit wavy line, where each wave correspond the entire cycle of economic development (Fig. 3).

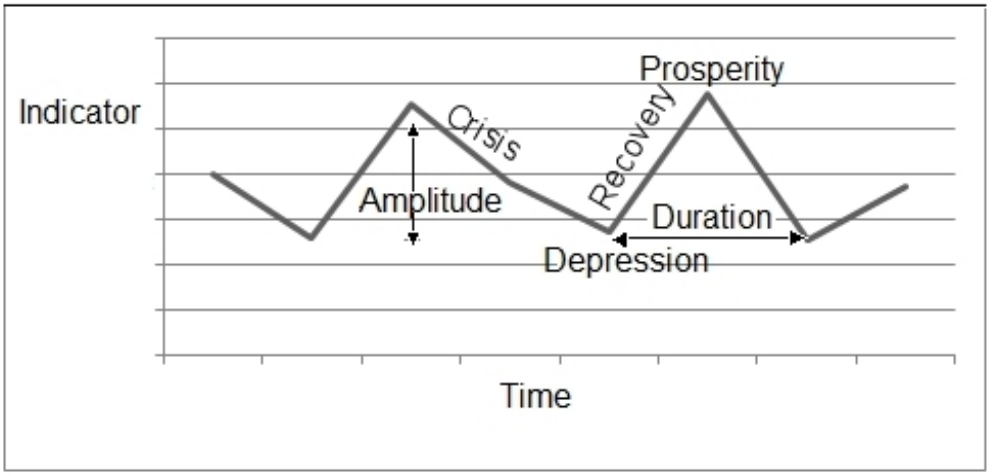

Fig. 3 - Graph of economic indicator cyclicality

In the middle 20th century (1946) R. N. Elliott examined economic fluctuations in a new. The main difference of his terminology is that each complete wave is the subwave of a larger next wave so periodicity is not. The mathematical foundation of his theory was the Fibonacci numbers (each number in the sequence equal to the sum of the preceding two numbers). The full set of waves any cycle is one of the elements of the Fibonacci numbers (Fig. 4) [14].

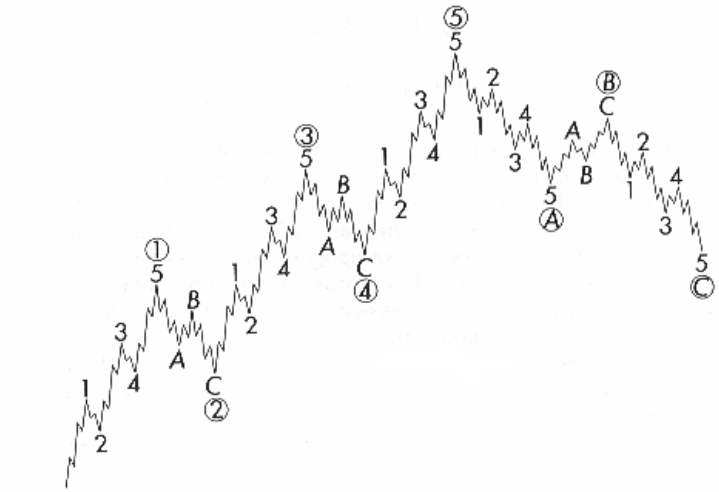

Fig. 4 - Schematic illustration of Elliott's waves

M. D. Kondratiev considered that process of real dynamics is only one. But this process is not straightforward, is not a simple upline, conversely, it is uneven, with shocks, vibrations of upline [10]. He was the first who prove that there are large cycles. It's important and essential fact of economic dynamics, which found reflection in all major areas of social and economic life. To justify his theory M. Kondratiev analyzed the development of economic indicators in dynamics: average commodity prices, loan interest, salary of industrial workers, volume of foreign trade turnover, production and consumption of coal, iron, lead, gold. For the analysis he used the statistical data of four leading capitalist countries: Britain, France, Germany, USA.

As a result of the performed researches it has been identified up-wave and down-wave in the structure of large cycles:

- the first cycle: 1787–1814 — up-wave, 1814–1851 — down-wave;
- the second cycle: 1844–1875 — up-wave; 1870–1896 — down-wave;
- the third cycle: 1896–1920 — up-wave.

Based on the theory of Kondratyev's long waves, it can be concluded that the development of scientific and technological progress is characterized by periodic fluctuations with 50-60 years cycles. Over the past centuries in the history of technological and innovative evolution there were observed five waves, that's why five technological modes were formed.

The first mode (1780-1830) was based on new technologies in the textile industry. The second (1830-1890) mode was associated with the development of rail transport and mechanization of the production of almost all types of products on the basis of the steam engine. The third (1880-1930) mode was based on the use of electricity in industry, the development of heavy engineering on the base of use of hire, studies in chemistry. The fourth (1930-1990 pp.) mode assumed the further development of energy, which was based of mainly on the use of oil and oil products, gas, communications, new synthetic materials. Industrial leaders of the fourth mode: the production of automobiles, aircrafts tractors and weapons. The fifth mode was assumed the use of achievements in the field of microelectronics, computer science, biotechnology, genetic engineering, new energy, space exploration, satellite technology.

It should be noted that research and analysis were conducted under capitalism conditions. Modern cycles differ from classical through regular practice of active state intervention in the economy and influence of advanced achievements of scientific and technical progress on economic activity.

Modern scientists determine the economic cycle, as the time interval between two states of the same quality of the conjuncture or as fluctuations of level of economic activity when periods of upturn changes periods of downturn [11].

N.V Krasnokutska [12], A.A. Kharin, I. L. Holenskyy [13] and T.P. Blyznyuk [14] think that cyclicality is a total form of movement of the national economy and the world economy as a whole which supposes changing of revolutionary and evolutionary stages of economic development, economic and progress expresses unevenness of functioning of the various elements of the national economy.

Modern economic science has more than 1,380 types of cycles, among which are the following (Table II).

Schumpeter suggested to combine static balance system with the theory of economic growth as a consequence he raised the equilibrium approach to a new evolutionary dynamic level. Schumpeter's hypothesis is based on the explanation of such factors as technical innovations that violate the previous balance and cause uneven development of economic events. The entrepreneur, who embodies innovation first, gets excess profits. If other entrepreneurs embody such innovation again the profit decreases. As a consequence, equilibrium is established at a new level. There is a decline in the old industries when introducing in production, but after some period of time new areas are expanded rapidly.

B. C. Ilyasov in his article [15] proposed the definition of the notion of false cyclicality, which can arise after the choice of the model, which is inadequate in relation to the studied process. For example, unreasonable choice of polynomial approximation and smoothing of data by using "moving average" that led to the fact that several cycles were received as the result of modeling. Thus, wrong cyclicality can become the source of unsubstantiated taking decision to economic management.

Cyclical fluctuations of economic indicators under the influence of various factors lead to the new state of the economic object. Natural transitions from one state to another form the economic behavior of the object, that is important as for individual businesses and for the economy as a whole.

TABLE II
TYPES OF ECONOMIC CYCLES [10].

Name of the cycle	Duration, years	Driving force
Kondratiev's cycle	40–60	Radical changes in the technological base of social production and restructuring
Kuznets's cycle	15–25	Shifts in the structure of reproduction of production
Zhuhlyar's cycle (Average economic cycle)	7–11	As a result of the interaction of many monetary and credit factors.
Kitchyn's cycle (Short cycle)	3–5	Dynamics of relative amount of stocks of materials in the enterprise
Private economic cycle	1–12	Fluctuations of investment activity
R. Lukas's balanced business cycle	-	Cycles are based on unexpected cash flows
A. Stokmen's "Real economic cycles"	-	Fluctuations of potential gross national product, which are caused on changes of taste, fashion, technological shifts. If these changes are temporary, they cause periodic fluctuations. If changes are long-term, they contribute to economic growth.

On the basis of analysis of various scientists works it can be assumed that certain factors influence on the economic behavior of the object and this leads to such phenomena as cyclicality. This leads to a need to consider the relationship between these two categories (Fig.5).

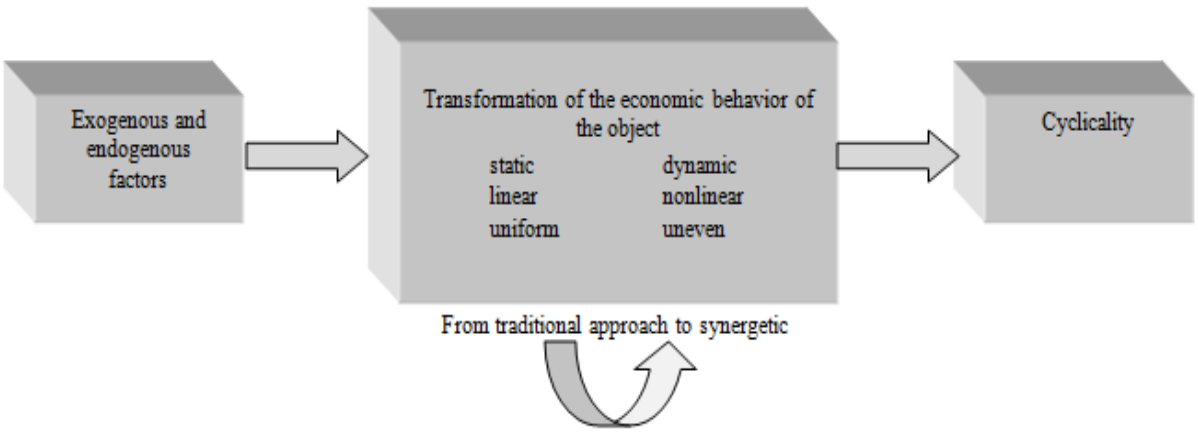

Fig. 5 – Relationship between cyclicality and economic behavior of the object

This picture shows that the economic behavior is under the influence various factors internal and external environment, properties of the economic system are changed which leads to the cyclicality.

IV. CONCLUSIONS

Thus, cyclicality of economic behavior of the object can be defined as "the process of changing of states of economic object that is repeated in varying degrees in time near point of equilibrium and can be caused by technical innovations, changes of cash flows, fluctuations in investment activity, structural reorganization of social production and that expresses uneven,

nonlinearity and dynamic of processes of development of the economic system". Later cyclicality can be the basis for building a model that it will provide an opportunity to substantiate expediency of making decision on effective management of the enterprise under the current economic conditions.

References

[1] F. M. Uzdenova. The “Constructs” of Modern Economic Cyclomatics. Journal of Scientific Publication: Economy & Business, 2010, Vol. 4. Part 4, pp. 12-27.

[2] F. M. Uzdenova. Spline-predicting of the behavior regional entrepreneur in russian economic realities. Modern problems of science and education, 2013. No. 1. URL: http://www.science-education.ru/ru/article/view?id=8216 (Accessed: 18 December 2015).

[3] V.A. Bessonov. Introduction to the analysis of the Russian macroeconomic dynamics transition. Moscow, 2003, 151 p.

[4] E.M. Chetyrkin. Statistical methods of forecasting. Moscow.: Statistics, 1977, 200 p.

[5] M.M. Butakova. Economic forecasting: methods and techniques of practical calculations: a tutorial. Moscow: Knorus, 2010, 168 p.

[6] W.S. Jevons. Investigations in Currency and Finance. — L., 1884, 428 p.

[7] Financial and economic dictionary. Available at: http://www.ivteme.ru/uk/glossary/financial—uk/ts—tsina+zak/tsiklichnist.html (Accessed: 19 December 2015).

[8] Ozhegov's Explanatory Dictionary. Available at: http://www.ozhegov.ru/slovo/58561.html (Accessed: 9 May 2015).

[9] A.J. Frost, R.R. Prechter. Elliot wave principle. Key to Market Behavior. ISBN: 0471988499. Wiley, 2001, p. 240.

[10] N.D. Kondratiev, Y.V. Yakovets, L.I. Abalkin. Big cycles of conjuncture and the theory of foresight. Selected works. Moscow: Economics, 2002, 550 p.

[11] V.N. Tarasevich. Economic theory. Tutorial. ISBN 966-364-185-1, Kiev, 2006, 784 p.

[12] N.V. Krasnokutskaya. Innovation Managemen. Tutorial. Kiev, 2003, 504 p.

[13] A.A Haryn, I.L Kolenskyy; E.Y. Shlenov. Innovation Management: The 3 books. Book 1. Fundamentals of innovative processes: tutorial. Moscow, 2003, 252 p.

[14] T.P. Blyznyuk. Theoretical aspects of the theory of N. Kondratiev’s long waves. Industrial economics, 2005, No. 1, pp. 11-18.

[15] R.H. Il'jasov. Phase analysis as a method of detecting of cyclicality in the economy. Modern high technologies, 2009, No. 1, pp. 32-36.

Development the Mathematical Models for Prediction the Content of Alloying Elements in Structural Steel During Ladle-Furnace Process

A.V. Zhadanos, I.V. Derevyanko

***Abstract*—**Regression models of silicon, manganese and carbon content behavior in metal depending on the amount of added carbonaceous materials, silicomanganese SiMn17, ferrosilicon FeSi65 are obtained as a result of analysis the experimental data for structural steel. These models enable to forecast the chemical composition of melting steel in order to save reducing agents and alloying elements. The structural diagram of automated information system of ladle-furnace is designed according to results of investigations.

I. Introduction

The permanently increase of requirements to quality of smelted steel causes the widespread introduction of secondary metallurgy. One of the main facilities of secondary metallurgy is a ladle-furnace, which is designed for desulphurization, alloying, deoxidizing metal and heating it to subsequent process steps.

The most important problem at the stage of structural steel treatment on the ladle-furnace is to provide stable regulated chemical composition of metal and rational charge of alloying and reduction alloys when steelmaking. According to current technology, at ladle-furnace treatment the chemical composition of steel is controlled only by mechanical sample taking and subsequent analysis in the laboratory. Therefore it is important to have data about element concentration behavior in the processed metal and to define the rational charge of alloying and reduction alloys based on these results. One of areas of this problem solution is working out of mathematical model for forecasting the final content of elements in the melt. There are two types of models that characterize the content behavior of chemical elements in metal during steel out-of-furnace treatment: physic-chemical based on thermo chemistry and thermo kinetics laws and regression models.

II. Retrospective of Researches and Publications

The advantage of the first models is a high accuracy of forecast [1-5], but structural of such models needs rather complicated calculations. At the same time, actual values of counted magnitudes do not coincide with theoretical ones which require their subsequent correction based on obtained experimental data. Regression models are less accurate, however it is possible to obtain data meeting the requirements to forecasting steel chemical composition at their application [6]. Regression models of Cr, Si, Mn and C contents behavior in bearing steel depending on the amount of added alloying and reduction alloys (carbonaceous materials, ferrosilicomanganese SiMn17, ferrosilicon FeSi65, ferrochromium FeCr800) during treatment in ladle-furnace are obtained [7]. Given the fact that the requirements for the content of alloying elements in structural steels are in a rather wide range, for example the steel for railway wheels contains according to standard GOST (interstate standard for Commonwealth of Independent States) 10791-2004 (0,55-0,65% C; 0,5-0,9% Mn; S 0,02%; 0,22-0,45% Si; P 0,02%; Ni 0,03%;

A.V. Zhadanos, 1- National Metallurgical Academy of Ukraine, Dnepropetrovsk, Ukraine,(email: Alexjad@mail.ru)
I.V. Derevyanko,1- National Metallurgical Academy of Ukraine, Dnepropetrovsk, Ukraine, (email: Ihorsic@meta.ua)

Cu 0,03%; H $2 \cdot 10^{-4}$ ppm [8]) it is reasonable to develop the regression models of alloying element content change in the process of structural steel treatment on the ladle-furnace in order to save reduction alloys and alloying ferroalloys.

III. The Development of Regression Models

The following materials are used for reducing and alloying of wheel steel: ferrosilicon of grade FeSi65 (63-68% Si) DSTU (state standard of Ukraine) 4127-2002 [9], silicomanganese SiMn17 (Mn 65%, 15-20% Si) DSTU 3548-97 [9] and carbon in the form of electrode breakage. Data of industrial smelting operations are processed by following parameters in order to construct regression models:

- weight of metal in the ladle M_{melt} = 105-115 tons;
- content of Si, Mn, C in metal-semiproduct prior to ladle-furnace treatment;
- weight of ferrosilicon FeSi65, silicomanganese SiMn17, carbon, kg - $mFeSi65$, $mSiMn17$, mC;
- content of Si, Mn, C in steel upon completion of ladle-furnace treatment, %: $[Si]_{fin}$, $[Mn]_{fin}$, $[C]_{fin}$;
- change of Si, Mn, C content in steel according to results of ladle-furnace treatment, %: $\Delta[Si]$, $\Delta[Mn]$, $\Delta[C]$.

Data of 28 smelting operations of wheel steel are approximated by linear regression equations using personal computer [10]. The following model is suggested for estimation of silicon content change:

$$\Delta[Si]=a_1 \cdot mFeSi65+a_2 \cdot mSiMn17+a_3, \tag{1}$$

where a_1, a_2, a_3 - equation factors, $[\%Si]$ - silicon content when current melt alloying.
Estimation of effect (significance) of regression equation factors on change of silicon content $\Delta[Si]$ by Student criterion is carried out. *T-statistics* values for each factor of equation are defined by the following equation [11]:

$$t_{a_j}=\left|\frac{a_j}{s_{a_j}}\right|, \tag{2}$$

where a_j - estimation of j - regression factor, s_{a_j} - estimation of average quadratic deviation of regression factor.
Estimation of average quadratic deviation of regression factors is carried out as follows [9]:

$$s_{a_j}=\frac{s_{rem}}{\sqrt{\frac{\sum_{i=1}^{n}(x_{ji}-\bar{x}_j)^2}{n}} \cdot \sqrt{n-m-1}}, \quad s_{a0}=\frac{s_{rem}}{\sqrt{n-m-1}}, \tag{3}$$

where n – volume of sampling, m – number of input variables in equation, s_{rem}^2 – estimation of remainder variance.

$$s_{rem}^2 = \frac{1}{n-m-1}\sum_{i=1}^{n}[y_i - f_i]^2 . \quad (4)$$

We compared obtained *T-statistics* values of factors to critical value *tcr* which is defined depending on number of degrees of freedom $k = n - m - 1$ and significance value $\alpha = 0.95$ under special tables or is computed on PC [9]. If $|t_{aj}| \geq t_{cr}$, regression equation factor is considered significant.

T-statistics values of equation (1) factors are as follows: $t_{a1} =$ 18.7; $t_{a2} =$ 5.3, $t_{a0} =$ 5.5. As *t-statistics* values of all factors are more than critical $t_{cr} =$ 1.98, all equation factors are significant and considered in equation.

Regression model adequacy by Fisher's ratio test is also estimated. F - statistics value is computed from equation 6 [11].

$$F_{calc} = \left(\frac{S_{regr}}{S_{rem}}\right) \cdot \left(\frac{k_2}{k_1}\right), \quad (6)$$

where $k_1 = m$, $k_2 = n - 2$ degree of freedom.

If *Fcalc* outnumbers the critical value of Fisher distribution *Fcr*, the equation is significant. As a result of calculations [9] we obtained the following values $F_{calc} =$ 195 and $F_{cr} =$ 3.1 (α = 0.05), i.e. equation (1) is significant and numerical values of factors $a_1 = 3.2 \cdot 10^{-4}$, $a_2 = 12.6 \cdot 10^{-5}$, a_3 = -0.039 (Figure 1). Determinacy factor r^2 of developed model is 0.82 and absolute accuracy of forecast – 0.06 %

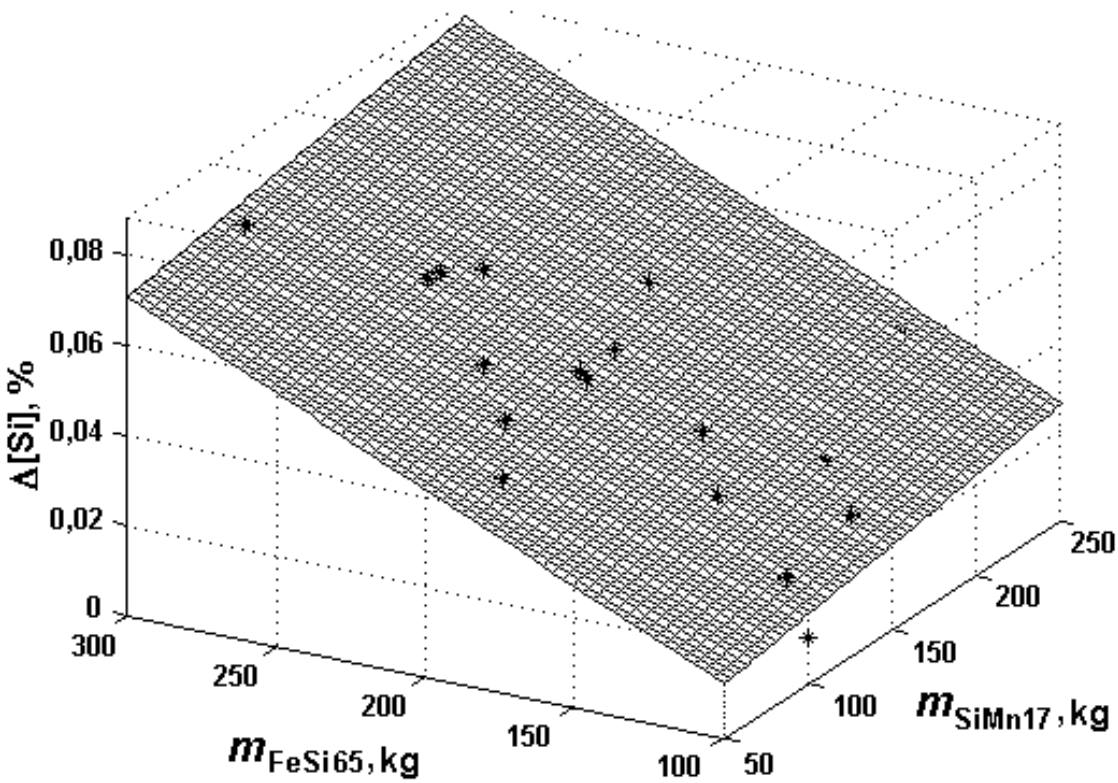

Fig. 1 Dependence of Si content change in structural steel for railway wheels during ladle-furnace treatment on specific charge of m_{FeSi65} and m_{SiMn17}: points - rated values of smelting operations, plane – obtained model

Regression model of manganese and carbon content change is obtained in a similar way. The models have determinacy factors r^2 are 0.81 and 0.73 accordingly. The absolute accuracy of forecast for [Mn] is 0.05 % and for [C] is 0.03%. It complies with the requirements for models.

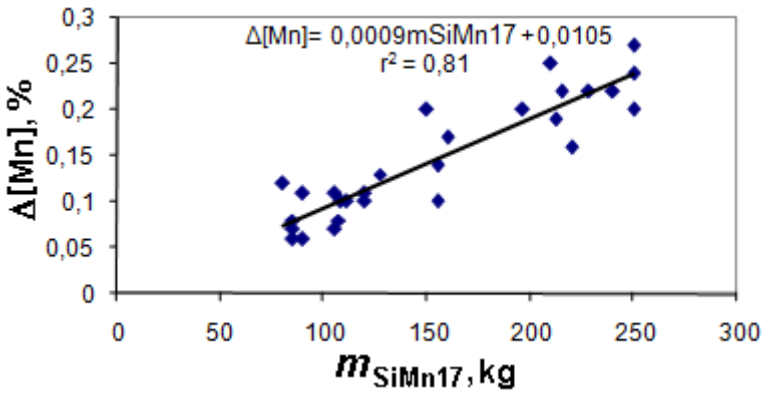

Fig. 2 Dependence of Mn content change in structural steel for railway wheels during ladle-furnace treatment on specific charge $m_{MnC17_{sp}}$: points - rated values of smelting operations, plane – obtained model

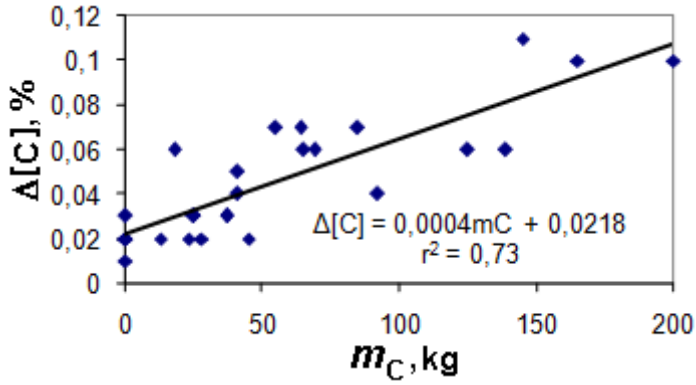

Fig. 3 Dependence of C content change in structural steel for railway wheels during ladle-furnace treatment on specific charge of carbon materials: points - rated values of smelting operations, plane – obtained model

IV. The Block Diagram of the Automated Information System

To implementation the developed models proposed automated information system (AIS) as a part of the observable automated control system of ladle-furnace (Fig. 4).

The main purpose of AIS is to give the operator at the control panel the current content of carbon ($[C]_t$), Si ($[Si]_t$), Mn ($[Mn]_t$)) in the metal during ladle-furnace treatment and recommendations about quantity of chemical additives, which necessary to add in the melt C ($m_{C_{rec}}$), FeSi65 ($m_{FeSi65_{rec}}$), SiMn17 ($m_{SiMn17_{rec}}$). AIS consists of the following subsystems: "predict of $\Delta[C]$"; "predict of $\Delta[Si]$"; "predict of $\Delta[Mn]$; "calc. of $[C]_t$"; "calc. of $[Si]_t$"; "calc. of $[Mn]_t$". "Recommendations about mSiMn17»; 'Recommendations about mFeSi65", "Recommendations about mC". The input parameters of the system are: $[Si]_{init}$, $[Mn]_{init}$, $[C]_{init}$, (the results of measurements enter to the system of mathematical models through a

programmable microprocessor controller); the amount, time and kind of added to the melt chemical additives, m_{Ct}, m_{FC65t}, m_{MnC17t}, the aim values of content Si, Mn, C - $[Si]_{fin.aim}$, $[Mn]_{fin.aim}$, $[C]_{fin.aim}$, (setting by the operator PPC). The above mentioned input and output subsystems' parameters, together with the results of the intermediate measurements additionally transferred to the subsystem "Backup". In case of technological changes of ladle-furnace process, the availability of subsystem "Backup" allows to perform automatic correction of model coefficients, embodied in the subsystems of automated information system. AIC is realized by integrating into existing process control system industrial computer with developed mathematical models.

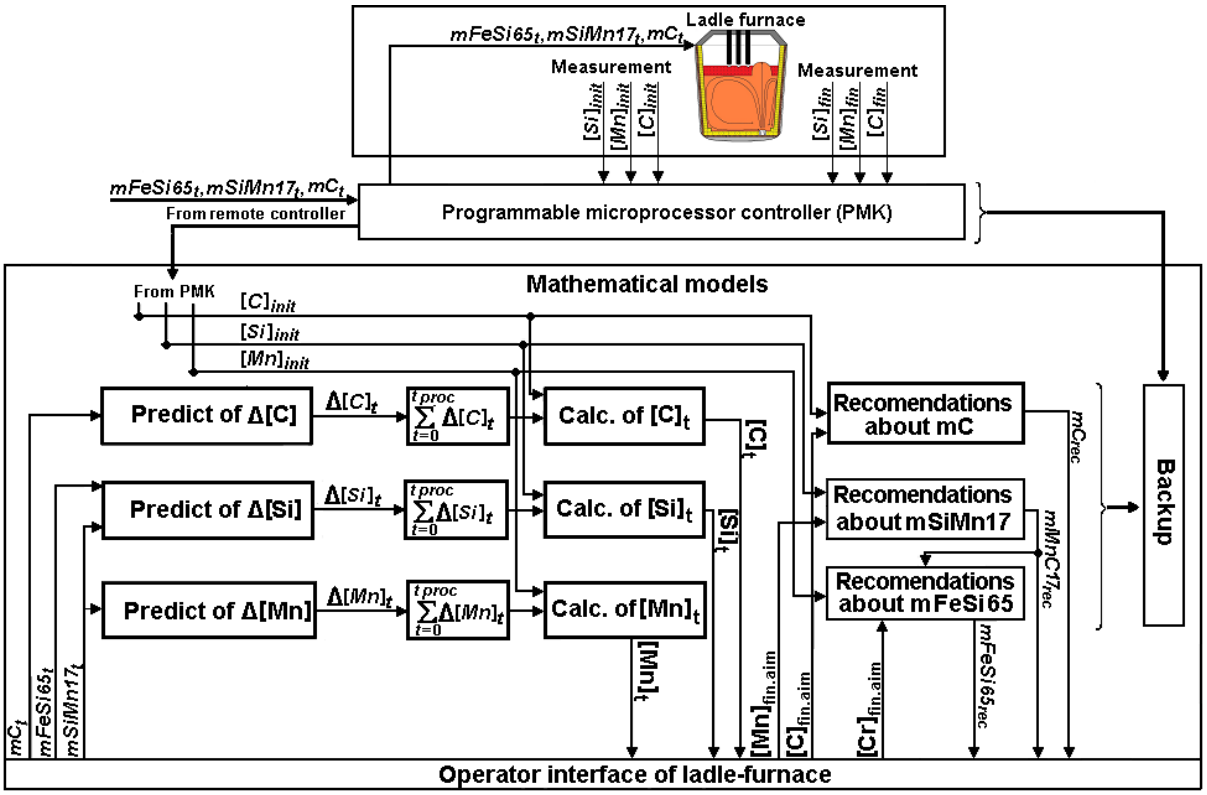

Fig. 4. The block diagram of an automated information system for monitoring the chemical composition of structural steel for railway wheels during processing in ladle-furnace based on developed models

V. Conclusions

1. Developed regression models of alloying elements content change in the process of structural steel for railway wheels treatment using ladle-furnace enable to forecast the concentration of Si, Mn and C in steel.

2. The structural diagram of AIS is made for implementation in the automation control system of secondary steelmaking. The main purpose of the system is monitoring of steel chemical composition and to issue the recommendations about the rational amount of alloying and reducing alloys.

References

[1] Industrial development of computer control of steel smelting at BMP and MMP, based on physic chemical model ORACLE. A.G. Ponomarenko, M.P. Gulyaev, I.V. Derevyanchenko, et al. Proceedings of Fifth Congress of Steelmakers, Rybnitsa (October 14-17, 1998), Moscow, Chermetinformatsiya, 1999, pp. 174-177. Published in Russian

[2] Prediction the composition of steel melts during smelting and secondary treatment. S.V. Kazakov. Metal i Litye Ukrainy, 2005, No. 3-4, pp. 17-20. Published in Russian

[3] Snegirev, Yu.V., Tutarova, V.D. and Fedorova, A.A. Using artificial neural network to predict steel chemical composition during secondary treatment in ladle furnace. Software of systems in the industrial and social fields. 2014. - №1. p. - 41-48. Published in Russian

[4] Zora JANCÍKOVÁ, Pavel ŠVEC. Prediction of chemical composition of refining slag with exploitation of artificial neural networks. Cybernetic letters: informatics, cybernetics and robotics. ISSN 1802-3525. 2008. - №2.

[5] Physic-Chemical Properties Forecasting for Manganese Ferroalloy Production Slag. E. V. Prikhodko, D. N. Togobitskaya, A. F. Petrov, A. F. Khamkhotko, S. V. Grekov. Metallurgical and Mining Industry, 2010, Vol. 2, No. 3 – p.p. 186-192.

[6] Vihlevschuk V.A. Ladle finishing of steel / V.A. Vihlevschuk, V.S. Kharakhulakh, S.S. Brodsky. - Dnepropetrovsk: SSPC "System Technology", 2000 - 190 p.

[7] A.V. Zhadanos, M.I. Gasik A.I. Panchenko, A.S. Sal`nikov, L.M. Skripka. Mathematical Model of Roller-Bearing Electric Steel Chemical Composition Control on the Ladle-furnace. Metallurgical and Mining Industry, 2010, Vol. 2, No. 6 – p.p. 390-396.

[8] Solid-rolled wheels. Specifications: GOST 10791-2011. - Moscow: The Interstate Council for Standardization, Metrology and Certification, 2011. - 10 p.

[9] M.I. Gasik, N.P. Lyakishev. Physical-chemical and technology of electrical ferroalloys, Dnepropetrovsk, System Technologies, 2005, 448 p. Published in Russian

[10] Kukushkin O.N. Statistics in Excel / O.N. Kukushkin, S.V. Beitcun, A.V. Zhadanos - Dnepropetrovsk: National metallurgical academy of Ukraine, 2002. - 64 c.

[11] William J. Orvis. Excel for Scientists and Engineers. SYBEX Inc. Alameda, CA, USA ©1995. ISBN 0782117619. 508 p. Published in Russian

Porter advanced method for the Universal Decimal Classification

Fiodor Tretyakov, Liya Serebryanaya

***Abstract*—**Text classification is one the most valuable domain of Data Mining. It can helps identify a category of a text. Universal Decimal Classification (UDC) is wide-spread system at scientific world. UDC—is a category tree. Each scientific publication should be related to the class. In Belarus, publication acquires UDC code only in libraries of universities with librarian worker. This article dedicated to automation of this task. For now, there is doesn't exist analogue of automated decimal classification.

***Keywords*—** Porter stemming, TF/IDF, Data Mining, Universal Decimal Classification.

I. Introduction

Today, there are large number of disordered text information. Therefore, a search and a classification of the information by keywords are the most important tasks. It is too actually, because researchers often have to read a lot of scientific articles, before finding something important for them. Sometimes they can just look for an article, to identify its sense, and, sometimes, that is necessary to read most of the text to understand its meaning.

Dewey #	10 Main Classes	Kinds of Books
000-099	General Works	encyclopedias, almanacs, record books, such as Guinness
100-199	Philosophy and Psychology	paranormal phenomena,such as ghosts, ethics, how we think
200-299	Religion	mythology, religions
300-399	Social Science	government, holidays, folklore, fairy tales, education, community
400-499	Language	English and foreign languages, sign language, dictionaries
500-599	Natural Science	math, chemistry, biology, weather, rocks, plants, animals in nature
600-699	Applied Science	inventions, health, drugs, transportation, cooking, pets
700-799	Fine Arts and Recreation	crafts, art, drawing, painting, music, games, TV, movies, sports
800-899	Literature	short stories, poetry, plays, jokes, riddles (fiction could be here)
900-999	History and Geography	countries, flags, historical events, biographies (92 or 920)

Fig. 1 UDC table

To identify a class of an article, it was invented Universal Decimal Classification (UDC). It is a mandatory attribute of any printed scientific work. With UDC it is easy to classify the

F. Tretyakov, Belarussian State University of Informatics and Radioelectronics, Minsk, Belarus, (e-mail: Fiodor.Tretyakov@gmail.com)
L. Serebryanaya, Belarussian State University of Informatics and Radioelectronics, Minsk, Belarus, (e-mail: l silver@mail.ru).

information in the world of science, literature and art, periodicals, different kinds of documents and scientific articles [1].

Currently, UDC is assigned manually at librarians or specially trained people. This article dedicated to methods and models to automatically assign the UDC, without involving humans. Therefore, the purpose of the work can be defined as the automation of the Universal Decimal Classification (Fig. 1).

II. Ways to Solve a Problem

The objective is to assign for each text from n texts a category m with UDC.

Subject of research work is Universal Decimal Classification of texts.

There are a lot ways to solve the problem. At first, there is should be defined resolving rule and a dividing function. The system processes texts and searches metrics, which will be substituted as parameters in the dividing function, and as a result text will be related to one of classes.

One of the significant factors influencing the choice of the class is the language of the text [2]. This article deals it with Russian text. Therefore, to build a classification algorithm, there are will be used features of Russian language.

One of the most popular ways of classification is to find the full match. However it can born the collision. For example, the user specifies the search word koshka (cat—in English). So, in the text or in the set of texts will be highlighted words which consist of a koshka (cat) and any extension of the word. This search is clear, but it cuts off the results, which could be useful to the user. For example, words *koshachiy* (cat's), *kot* (cat). This method is the fastest, but with low accuracy. But software that will created based on this method will not real-time based, so high-performance is not main goal [3].

Russian language has difficult structure and a lot of word-parts. So, the situation, when two words should relate to one class is too often. And to increase accuracy, the best solution is to select a part of a word that reflect its sense. This can often be the root of the word, but it is difficult to select it. For example, some part of a word like a fugitive vowel can't be easy separated, so it decreases accuracy [4] [5].

III. Text parser module

Next past is a text parser module. To apply Stemmer, text should be split by words. It can be done by representing the text like a line and parse it by non-word symbols.

Not all words are significant for classification. They are called stop words. There are removing prepositions and erroneous words.

Another thing is help the system to select keywords—is the Zipf's Law. It allows to exclude words that has no sense for processing. There are words that misspelled, word-parts and so on. There is an algorithm of keyword finding:

1)Split text t by words by ". , ! ? space tab line end".

2)Remove non-valuable words by stop word dictionary multiplying (just vector multiplication).

3)Select keywords by Zipf's law.

IV. Classification module

The next step is to create a classification module.

The classification method will be based on the Stemmer.

The UDC represented like a tree and consists of 126 441 categories. This is too much to start a classification directly. This method will has to low performance and to avoid it, it is a great

improvement to use embedded feature of UDC—the hierarchy. The searching of a category reduces to passing the tree. But it require the special tree extension of tree—the siblings. So the algorithm will be built as following:

1) There is the processing of descriptions of all categories with the module by extracting the roots of words and put the result in the word dictionary. Every line in this dictionary is a key, which is the root of the word, and the value in a row—the number of word forms by a key from the description of the category.
2) Complete the Step 1 for all texts, applying them to these abstracts.
3) Select the initial list of categories. Let it be the children of the invisible parent category (the root UDC category).
4) Select begging category set. Its number is determined by the value of the variable T, calculated by formula 1.
5) There is a variety of categories for the text, where T is the maximum. If such T more than 1, then the system will process all trees parallel the result is the UDC-code connected by + a list of categories.
6) When this category has a subcategory, next searching set is a category's children plus the category, because the text could refer to it. This case method goes to step 7. If subcategories do not exist, the algorithm ends.
7) Look T for selected categories. If the largest T-value for the parent, then select it and finishes the algorithm. If subcategory "wins" (T-value for it is maximal), the system goes to step 6.

$$T = \sum_{i=0, j=0}^{n,m} A_i \times B_i$$

V. TF/IDF ALGORITHM

Tf–idf, short for term frequency–inverse document frequency, is a numerical statistic that is intended to reflect how important a word is to a document in a collection or corpus. It is often used as a weighting factor in information retrieval and text mining. The tf-idf value increases proportionally to the number of times a word appears in the document, but is offset by the frequency of the word in the corpus, which helps to adjust for the fact that some words appear more frequently in general.

Variations of the tf–idf weighting scheme are often used by search engines as a central tool in scoring and ranking a document's relevance given a user query. tf–idf can be successfully used for stop-words filtering in various subject fields including text summarization and classification.

One of the simplest ranking functions is computed by summing the tf–idf for each query term; many more sophisticated ranking functions are variants of this simple model [2].

tf–idf is the product of two statistics, term frequency and inverse document frequency. Various ways for determining the exact values of both statistics exist.

In the case of the **term frequency** tf(t,d), the simplest choice is to use the *raw frequency* of a term in a document, i.e. the number of times that term t occurs in document d. If we denote the raw frequency of t by $f_{t,d}$, then the simple tf scheme is tf(t,d) = $f_{t,d}$.

- Boolean "frequencies": tf(t,d) = 1 if t occurs in d and 0 otherwise;
- logarithmically scaled frequency: tf(t,d) = 1 + log $f_{t,d}$, or zero if$f_{t,d}$ is zero;
- augmented frequency, to prevent a bias towards longer documents, e.g. raw frequency divided by the maximum raw frequency of any term in the document:

$$tf(t,d) = 0.5 + 0.5 \times \frac{f_{t,d}}{max\{f_{t',d} : t' \epsilon d\}}$$

The **inverse document frequency** is a measure of how much information the word provides, that is, whether the term is common or rare across all documents. It is the logarithmically scaled inverse fraction of the documents that contain the word, obtained by dividing the total number of documents by the number of documents containing the term, and then taking the logarithm of that quotient [3].

$$idf(t, D) = log \frac{N}{|\{d \epsilon D : t \epsilon d\}|}$$

with

- N: total number of documents in the corpus N = |D|
- $|\{d \epsilon D : t \epsilon d\}|$: number of documents where the term *t* appears (i.e., $tf(t, d) \neq 0$). If the term is not in the corpus, this will lead to a division-by-zero. It is therefore common to adjust the denominator to $1 + |\{d \epsilon D : t \epsilon d\}|$.

Mathematically the base of the log function does not matter and constitutes a constant multiplicative factor towards the overall result.

Then tf–idf is calculated as

$$tfidf(t, d, D) = tf\,(t, d) \times idf\,(t, D)$$

A high weight in tf–idf is reached by a high term frequency (in the given document) and a low document frequency of the term in the whole collection of documents; the weights hence tend to filter out common terms. Since the ratio inside the idf's log function is always greater than or equal to 1, the value of idf (and tf-idf) is greater than or equal to 0. As a term appears in more documents, the ratio inside the logarithm approaches 1, bringing the idf and tf-idf closer to 0 [1].

VI. Results

Now it is necessary to compare the methods in the field of accuracy. In the case of absolute precision: the method of frequency classification based on the full-text search (A), the method of frequency classification using Stemming (B), the frequency method without the Stemming but with the ANN (C), frequency method using both the Stemming and the ANN (D), a semantic reference expert system (pseudo-reference confidence 90%) (E) (Fig. 2).

The graph shows that D (76%) is very close to the format of E. At the same time as the difference between B (47%) and C (50%) is not so much. Full-text frequency method gives the accuracy of only 23%. This chart reflects the confidence of the classifier with the choice.

If there are using relative accuracy, then it is E 97%, D show excellent results—90%. The difference between C and B increases—75% and 65% respectively. For A is—40%.

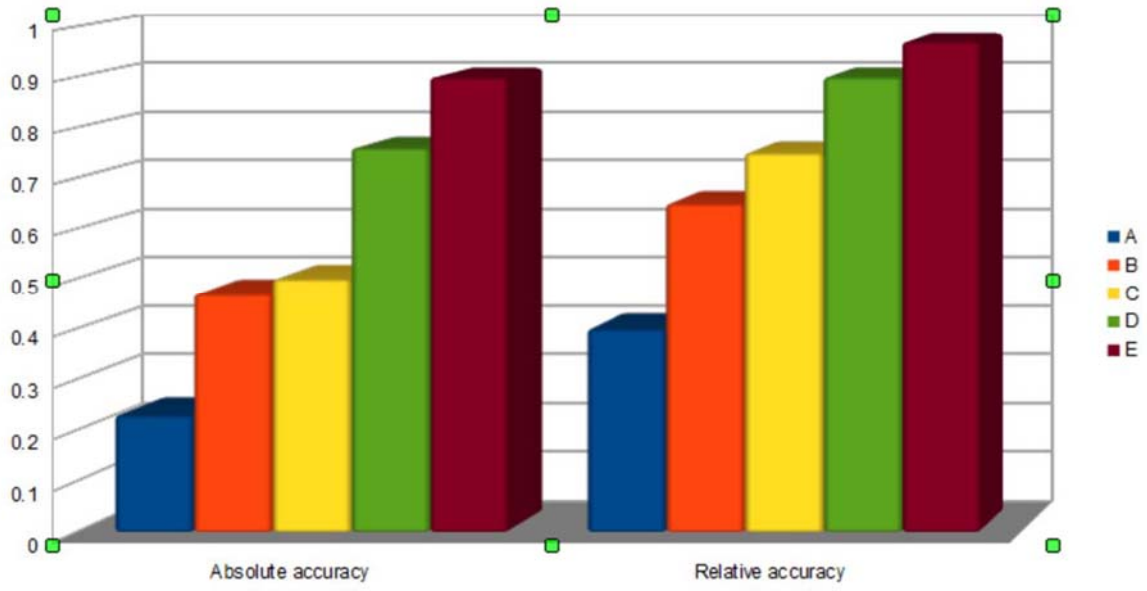

Fig. 2 Results

VII. Conclusion

With stemmer, texts can be classified with high accuracy. The minus is the complexity of the architecture of the module.

To demonstrate the performance of this algorithm must be integrated into a software package.

The package has the following specification:

1) Receive an input text.
2) Classify.
3) Push the text in the database with the appropriate index to account for this result in the following classifications.
4) Print the results to the user on the screen.

The result is a system that allows user to assign UDC to text with high speed, accuracy and it is automated.

Acknowledgment

The authors would like to thank to the Head of Belorussian State University of Informatics and Radioelectronics— Mikhail Batura, to the Head of Computer Systems and Networks Department, and to the Head of Software of Information Technologies Natalia Lapickaya.

References

[1] V. Tolstoy, “Deep analysis of the text. From the series of lectures "Modern Internet-technologies" for students of the 5th grade of the Department of Computer Technology Faculty of Physics”, Donetsk, Ukraine: Department of CS, 2005.
[2] F. Tretyakov and L. Serebryanaya, “Russian texts' classification method”, Minsk, Belarus: International scientific and technical conference dedicated to the 50th anniversary of the MRTI-BSUIR sourcebook, 2014.
[3] F. Tretyakov and L. Serebryanaya, “Automated method of universal decimal classification in the field of distance learning”, Minsk, Belarus: Distance Learning - Educational environment XXI century sourcebook, 2014.
[4] P. Braslavsky, “Favorite applied problems of computer science”, Moscow, Russia: Williams, 2005.
[5] R. Duda, P. Hart and D. Stork, “Pattern classification”, New-York, USA: John Wiley & Sons, 2001.

Development of the Support System for Analysis of the Correlation Psychological Characteristics and Signature Properties

Jan Rabcan, Petra Poklonova, Roman Behul

***Abstract*—**Project is focused on analysis of the correlation psychological characteristics and signature properties of person. Our goal is to propose method to find the correlation between psychological properties and signature of person. This paper summarizes the progress after first phase of our project.

***Keywords*—**psychological, signature, analysis, data mining

I. Introduction

The main reason, why we decided to work on this project is that everybody can clearly say a many features of his psychological character. In most cases people are not objective and unbiased. This fact is used in graphology. Graphology provides analysis of psychical character of person and patterns of a handwriting text to be able to make evaluating of personality characteristic. In our case, patterns of a handwriting text are signature of persons. The field of signatures is not very described. Lots of graphologists mean that analysis of signature is not sufficient [1 – 3]. It is the reason why lots of them are focused on handwriting text and signature together. A few authors who are attended on only signature are not in some definitions very clear but basically the field is not very explored. Importance of analysis of signature is noticeable especially in companies, which use to do this analysis during a job interview. Next important usage can be in medicine. For example, the system can be able to detect a stressed surgeon.

II. Suggested solution

The main aim of our project is finding to penetration of different graphologist meanings and find new context. The next important goal of the project is find some psychical properties and assign it to the signature properties. In final, we want to develop system, which takes signature of user, analyze the signature and after analysis it will be possible to show results to the user. Displayed result informs the user about his psychological characteristic and it can estimate the current state of person. For instance, current state can determine whether the user is angry now. Diagram in Fig.1 shows process from start to end.

At start we had to create tests. Tests are divided into two categories. First category is for psychological tests and the second one is for tests focused on signature. We had to make own psychological test, because the current legislation in this field of psychology is very strict and using of validate tests is charging. We assume, that our test get validate results too.

J. Rabcan, University of Zilina, Zilina, Slovakia (e-mail: jrabcanj@gmail.com).
P. Poklonova, University of Zilina, Zilina, Slovakia
R. Behul, University of Zilina, Zilina, Slovakia

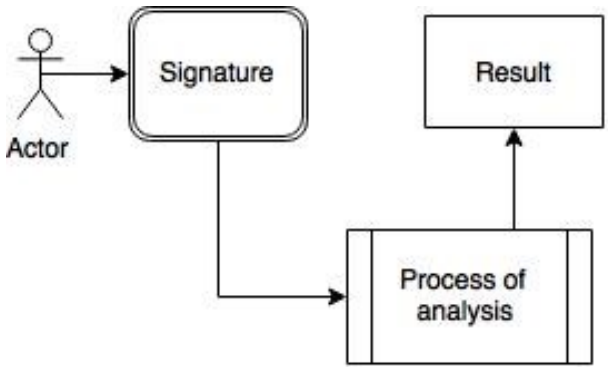

Fig. 1 Diagram of process

At first of all, we create the test which contains 167 questions. Questions in the test are separated in two groups. First group is focused on graphology and second group is focused on psychology. We try to collect a many results. According to the results we want to make the study. In study we want to find some correlation between psychological part of the test and graphologist part. We create a web page for collecting data. All results from tests are saved in database. Our page is written in PHP. Users can look into the help during the test. We used JavaScript for showing the help. The help explain some technical terms about signature. For explanation of terms, we used pictures. The page has responsible design. Our project includes two main *php* files. The first file is necessary for visualization of the questions and answers. The second file is for processed the test form.

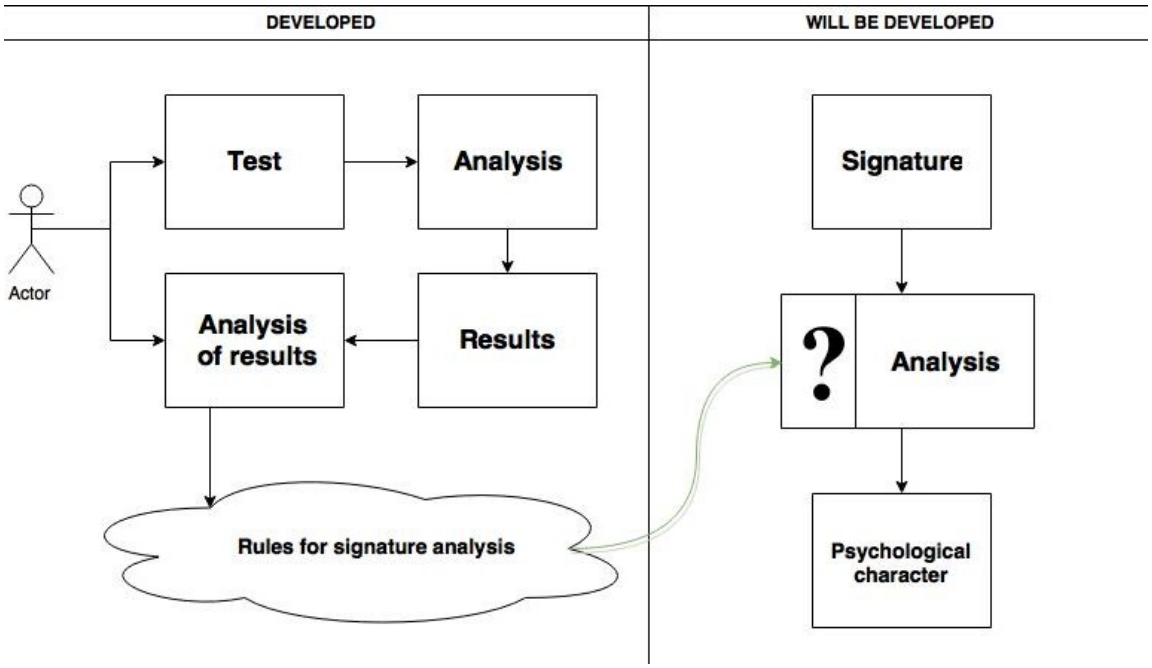

Fig. 2 Diagram of functionality and progress of development

III. Database design

All necessary information is stored in database. We used *MySQL* database. Database contains 9 tables. Database scheme is shown in Fig.3.

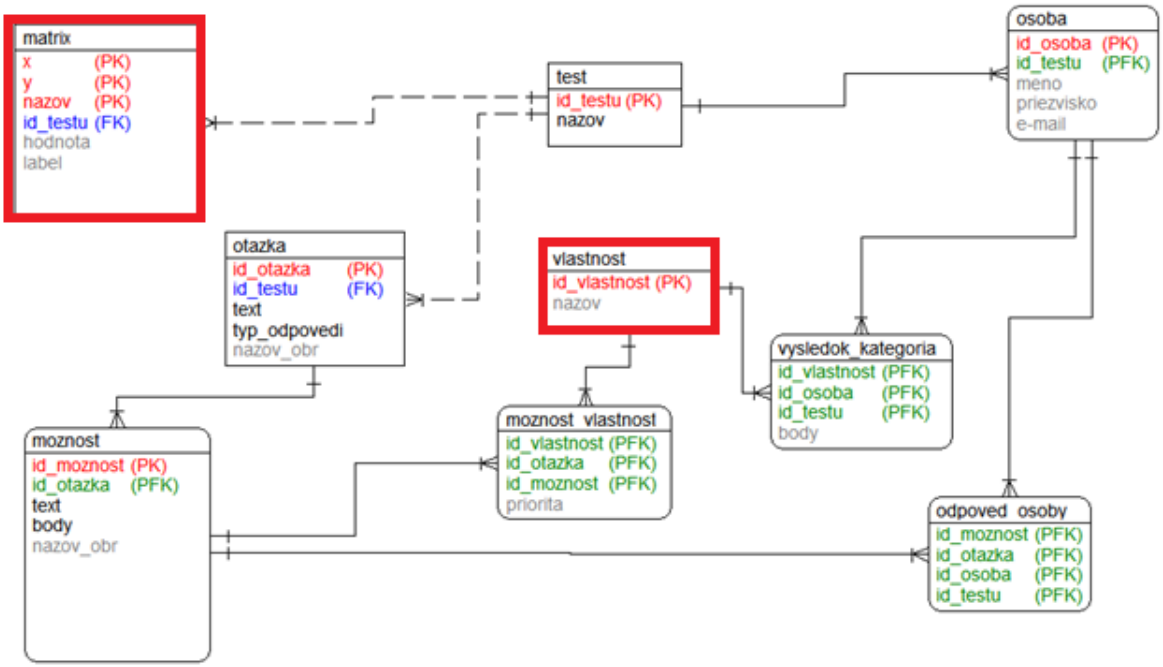

Fig. 3 ERA-model demonstrate the dependencies of entities. Selected tables are used for estimate psychological character of person.

Table *otazka* include all questions and according to attribute *id_testu* we can assign every question to the test, because every kind of test has own unique id number of identification. Tests are stored in table named *test*. All questions in test have assigned answers. Answers are stored in table named *moznost.* The main aim of tests is find some mutual psychological and graphological features of the person. These features are stored in table named *vlastnost.*

Users have to fill answers of questions. After click on confirm button the system creates a new record in table *osoba*. Then answers are stored in table *odpoved_osoby*. Next important event after on-click method is computes result of all categories of the psychology test. These results are stored in table *vysledok-kategoria.*

IV. Conclusion

In first phase of project we suggest system for collecting data and we proposed simple structure of our system. At next phase we can use collected data for analysis of person characteristics.

The presented result has been developed under special subject “Project” at the Faculty of Management Science and Informatics of University of Zilina (Zilina, Slovakia).

References

[1] M. Pokorný, “Synthetic Identification according to content hand writing” , Ed. University of Zlin, 2008
[2] J. BURGR, *Písmo odhaluje osobnost.* *Praha*, ISBN 80-86421-30-9, 2001.
[3] J. KULKA, *Grafologie*. Brno, 1991

Deep Learning Concept for Hyperspectral Imagery Classification

Sergey A. Stankevich, Iryna A. Piestova, Victor N. Podorvan

Abstract — The adaptation of deep learning concept for hyperspectral imagery classification is presented. The concept proposed a six-layer processing methodology, which includes a pre-processing, an optimal band selection procedure, both spectral feature-based and spatial feature-based land cover classification as well as land cover change detection process using formal schema.

Keywords — deep learning, hyperspectral imagery classification, band selection, change detection.

I. Introduction

Along with the technology development and the improvement of hyperspectral imagery both spectral and spatial resolution, the hyperspectral data requires a deeper analysis due to the increased amount and complexity of observable phenomena [1]. Representation and organization of multiple levels in order to express complex relationships among data defines a deep learning process. One of the promises of deep learning is replacing handcrafted features with efficient algorithms for unsupervised or semi-supervised feature learning and hierarchical feature extraction. Feature hierarchies are discovered considering that higher levels are formed by combining features from lower level [2].

II. Concept and methods

Deep learning is a branch of machine learning based on a set of algorithms that attempt to model high-level abstractions in data using multiple processing layers. For each level, models include complex structures or otherwise, composed of multiple non-linear transformations. This one must be developed according to the type of information desired, namely pixel-based, object-based or structure-based. In respect to the hyperspectral imagery analysis, the deep learning general methodology involves several sequential and parallel data processing levels [3]: pre-processing, band selection, preliminary classification – both spectral feature-based and spatial feature-based, class fusion as well as change detection if needs.

A. Pre-processing

Pre-processing level operations include geo-referencing, geometric, radiometric and atmospheric correction and can sometimes supplied by satellite imagery provider. In case of multiple images analysis initially they are matched using ground control points (GCP). Hyperspectral image digital numbers (DN) are converted into at-sensor spectral radiance using each-band calibration factors extracted from image metadata. Next, the atmospheric correction is performed and floating-point values of the surface spectral reflectance are obtained [4].

S. Stankevich, Scientific Centre for Aerospace Research of the Earth, Institute of Geological Science, National Academy of Sciences of Ukraine, Kiev, Ukraine (e-mail: st@casre.kiev.ua).
I. Piestova, Scientific Centre for Aerospace Research of the Earth, Institute of Geological Science, National Academy of Sciences of Ukraine, Kiev, Ukraine
V. Podorvan, Scientific Centre for Aerospace Research of the Earth, Institute of Geological Science, National Academy of Sciences of Ukraine, Kiev, Ukraine

B. Band Selection

These operations consist in selection of informative bands of hyperspectral image [5]. The $C(\lambda)$ informativity criterion is used for the hyperspectral imagery spectral bands selection in remote sensing applications [6]:

$$C(\lambda) = \frac{D(\lambda)}{4r^2(\lambda)} \cdot \log_2[1+\psi(\lambda)] \tag{1}$$

where $D(\lambda)$ is Kullback-Leibler divergence in the spectral space, $r(\lambda)$ is an equivalent spatial resolution of current spectral bands set, $\psi(\lambda)$ is an equivalent signal-to-noise ratio in target detection by multi-dimensional optical signal, λ is a spectral bands subset.

The best of spectral bands subset selection of hyperspectral image in terms of (1) criterion is an optimal search problem in hyperspectral image spectral bands combinations space. This problem can be solved using one of the known methods, e. g. pseudo-gradient search [7].

C. Spectral feature-based classification

Spectral feature-based classification is the analysis of object or material features by spectral values. This one detects desired target spectra in image for remote sensing applications.

One of the widely used algorithms such as support vector machine (SVM) [8] or spectral topological classifier (STC) [9] can be applied for classification by spectral features. The following equation described the classification rule for STC:

$$\Delta z = \frac{1}{m}\sum_{\lambda} |\operatorname{sign}(\Delta E_\lambda, \sigma_\lambda)| + \frac{1}{2(m-1)}\sum_{\lambda} |\Delta \operatorname{sign}\left(\frac{\partial E_\lambda}{\partial \lambda}, \frac{\partial \sigma_\lambda}{\partial \lambda}\right)| \tag{2}$$

where, $\operatorname{sign}(E,\sigma) = \begin{cases} 1 \text{ if } E > \sigma \\ 0 \text{ if } |E| \le \sigma \\ -1 \text{ if } E < -\sigma \end{cases}$.

D. Spatial feature-based classification

There is an object-oriented classification of image targets by spatial features. Especially the Radon transform can be used to detect image targets by its shape [10] or the Hough transform can be used to detect linear patterns [11].

Both classification types generate the corresponding preliminary probability maps for image objects. They are provided by a fundamentally different identification features.

E. Change detection

In remote sensing applications changes are considered as land surface component alterations. Change detection is the process of identifying and quantifying differences in the objects state using multi-temporal satellite images [12]. Post-classification comparison separately classified multitemporal images, pixel by pixel. Engagement classification maps instead raw images minimizes impacts of atmospheric, sensor and environmental differences between multitemporal datasets, as well as provides a complete matrix of change information [13].

III. Results and discussion

The methodology described in the previous section was applied to the hyperspectral satellite image analysis of territory Lekuk, Poland. The PROBA-1 satellite image by Compact High Resolution Imaging Spectrometer (CHRIS) was investigated (Fig. 1). CHRIS instrument provides 19 spectral bands (fully programmable) in the VNIR range (400 – 1050 nm) at a 17 m ground sampling distance (GSD) [14]. Two multitemporal source hyperspectral images were acquired in similar conditions for the same phase of vegetation phenological cycle.

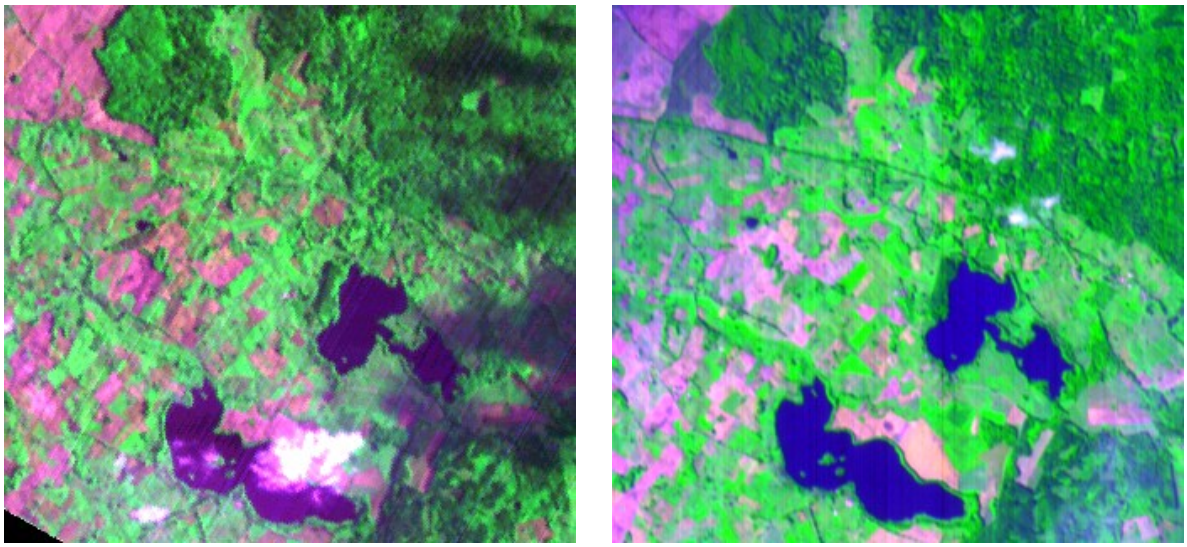

a *b*

Fig. 1 CHRIS hyperspectral satellite images (19 spectral bands, 17 m resolution, pseudo-natural color synthesized) of test site in Lekuk region (Poland): August 03, 2014 (*a*) and August 20, 2015 (*b*)

Pre-processing of the both images was performed, and then the two images were co-registered with pixel accuracy using GCP.

The process of optimal band selection using (1) criterion is illustrated by Fig. 2 diagram. Totally 11 spectral bands of 18 were selected for further analysis from the image of 2014 and 10 ones from 16 – from the image of 2015.

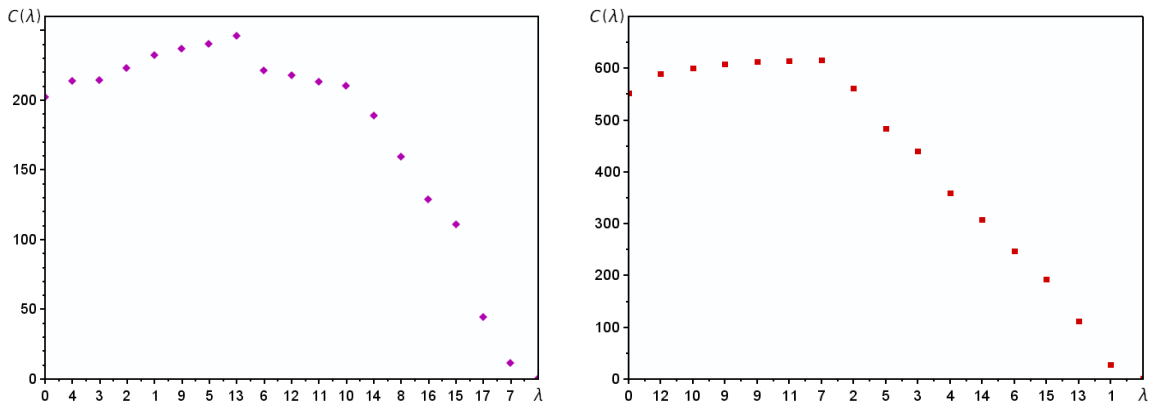

a *b*

Fig. 2 Optimal band selection for CHRIS hyperspectral imagery of test site in Lekuk region (Poland): August 03, 2014 (*a*) and August 20, 2015 (*b*)

Spectral-feature classification of land cover into eight primary classes of woodlands and farmlands was performed using the SVM algorithm (Fig.3) and STC (Fig.4). The weather

conditions greatly affect the classification results. It is best to use clean cloudless pictures. Otherwise, separate classes for clouds and cloud shadows were created. The area occupied by these classes does not participate in change detection process.

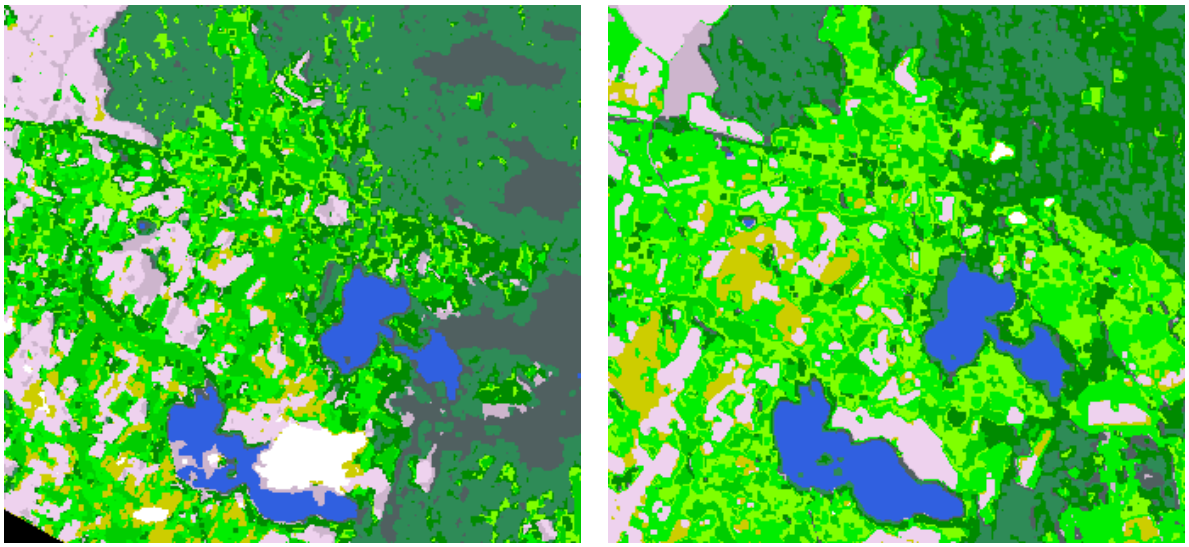

a *b*

Fig. 3 Land cover classification by SVM algorithm (12 unified classes) of test site in Lekuk region (Poland): August 03, 2014 (*a*) and August 20, 2015 (*b*)

Legend: – Unclassified, – Water, – Coniferous, – Deciduous, – Barren, – Cropland, – Sparse, – Meadow, – Grassland, – Cloud, – Shadows, – Wetland

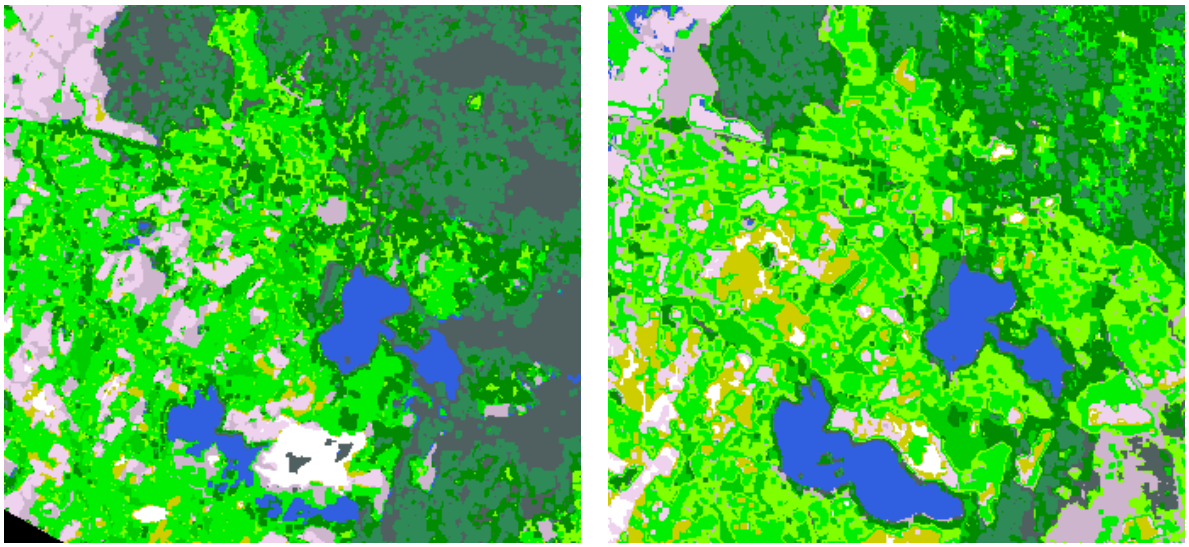

a *b*

Fig. 4 Land cover classification by STC (12 unified classes) of test site in Lekuk region (Poland): August 03, 2014 (*a*) and August 20, 2015 (*b*)

Legend: – Unclassified, – Water, – Coniferous, – Deciduous, – Barren, – Cropland, – Sparse, – Meadow, – Grassland, – Cloud, – Shadows, – Wetland

The SVM algorithm is more resistant to image noise and radiometric distortions. Vice versa, the STC more accurately separates the classes with complex spectra.

Since the objects under study haven't expressed geometric features, in this research the spatial-based processing performed as a post-classification by clumping.

After mapping of changes occurring at different-time land cover classifications of study area

(Fig. 3, Fig. 4) the spatial distribution of their importance has been obtained [15]. The expert pair-class estimate matrix is given in Table I.

TABLE I
EXPERT CLASS-CHANGE ESTIMATE MATRIX

Land cover	0	1	2	3	4	5	6	7	8	9	10	11
0. Unclassified	0	0	0	0	0	0	0	0	0	0	0	0
1. Water	0	4	7	7	5	5	6	6	6	0	0	6
2. Coniferous	0	1	4	4	1	2	2	3	3	0	0	2
3. Deciduous	0	1	4	4	1	2	2	3	3	0	0	2
4. Barren	0	3	7	7	4	5	5	6	6	0	0	6
5. Cropland	0	3	6	6	3	4	5	6	6	0	0	6
6. Sparse	0	2	6	6	3	3	4	4	5	0	0	4
7. Meadow	0	2	5	5	2	2	4	4	4	0	0	4
8. Grassland	0	2	5	5	2	2	3	4	4	0	0	4
9. Cloud	0	0	0	0	0	0	0	0	0	0	0	0
10. Shadows	0	0	0	0	0	0	0	0	0	0	0	0
11. Wetland	0	2	6	6	2	2	4	4	4	0	0	4

Evaluation of changes made based on the analysis of the impact occurring, or possible changes to the ecological status of the territory. The expert chooses the code of change, which is subdivided into 7 estimates: three negative, three positive and one neutral.

Both positive and negative changes were subdivided into three levels each for easy visualization, as shown in Fig. 5.

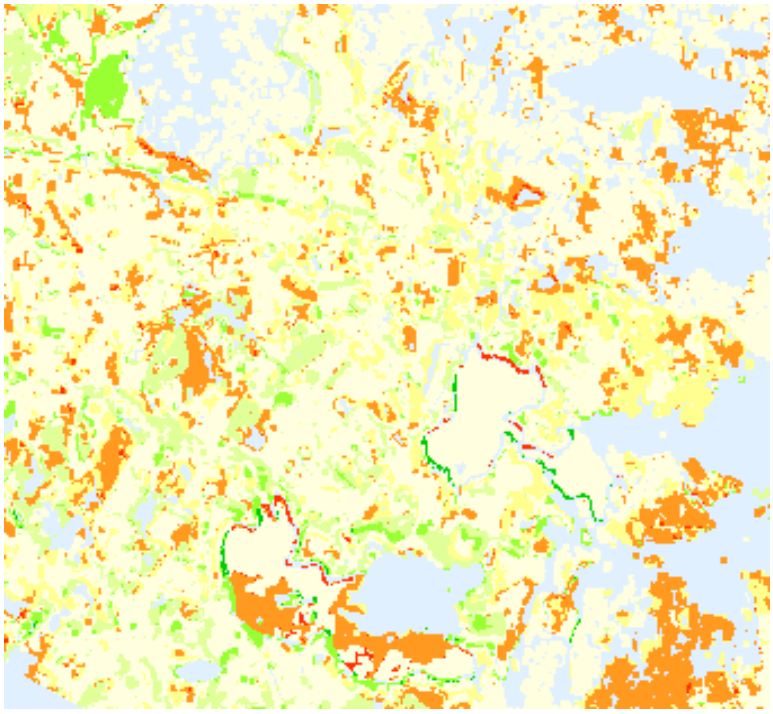

Fig. 5 Spatial distribution of land cover change estimates of test site in Lekuk region (Poland) during 2014-2015: in levels of importance.
Legend: – strong negative, – moderate negative, – weak negative, – neutral, – weak positive, – moderate positive, – strong positive

In accordance with the methodology described in paragraph 2, the process of classification of hyperspectral imaging is illustrated by dataflow diagram (Fig. 6). It consists of the following

layers: level 1 – input data, level 2 – pre-processing, level 3 – band selection, level 4 – classification, level 5 – change detection, level 6 – output.

Output level of Fig.6 is already suitable for use as a final data product remote sensing applications.

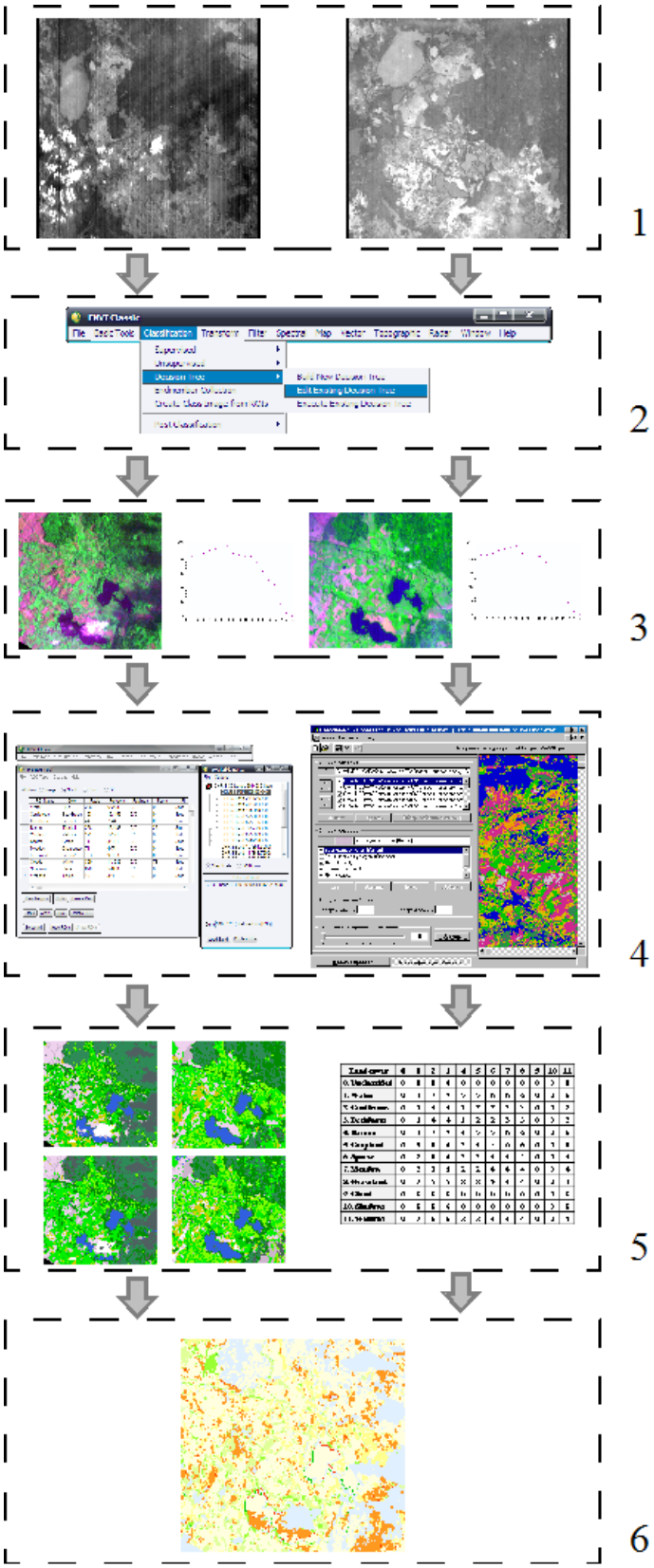

Fig. 6 Dataflow diagram for hyperspectral imagery classification based on deep learning concept

IV. Conclusion

Thus the deep learning concept for hyperspectral imagery classification methodology is proposed. The methodology includes six levels of hyperspectral imagery analysis, from raw hyperspectral image up to final data product.

The proposed concept is the basis for formalizing the hyperspectral imagery classification process. Such formalization is very important in developing the information systems for Earth's surface monitoring or the similar geospatial services [16].

References

[1] M. Dalponte, L.Bruzzone, L. Vescovo, D. Gianelle, "The role of spectral resolution and classifier complexity in the analysis of hyperspectral images of forest areas," *Remote Sensing of Environment*, vol. 113, pp. 2345–2355, November 2009.

[2] C. Vaduva, I. Gavat, M. Datcu, "Deep learning in very high resolution remote sensing image information mining communication concept," *Proceedings of the 20th European Signal Processing Conference (EUSIPCO)*, Bucharest, Romania, pp. 2506–2510, August 2012.

[3] J. Li, P.R. Marpu, A. Plaza, J.M. Bioucas-Dias, J.A. Benediktsson, "Generalized composite kernel framework for hyperspectral image classification," *IEEE Transactions on Geoscience and Remote Sensing*, vol. 51 (9), pp. 4816–4829, March 2013.

[4] G. Shaw, D. Manolakis, "Signal processing for hyperspectral image exploitation," IEEE *Signal Processing Magazine*, vol. 19 (1), pp. 12–16, January 2002.

[5] G. Petrie, P. Heasler, T. Warner, "Optimal band selection strategies for hyperspectral data sets," *Proceedings of IEEE International Geoscience and Remote Sensing Symposium*, Seattle, USA, vol. 3, pp. 1582–1584, July 1998.

[6] S.A. Stankevich, "Quantitative estimation of hyperspectral aerospace imagery informativity in remote sensing applications," *Reports of the National Academy of Sciences of Ukraine*, no. 8, pp. 53–58, August 2006.

[7] S.A. Stankevich, "Hyperspectral aerospace imagery spectral bands optimal selection in remote sensing applications," *Space Science and Technology*, vol. 13, No. 2, pp. 25–28, April 2007.

[8] J. Shawe-Taylor, N. Cristianini, "An Introduction to Support Vector Machines and Other Kernel-based Learning Methods," Cambridge University Press, 204 p, March 2000.

[9] M.A. Popov, S.A. Stankevich, V.N. Podorvan, "Software and technology for land cover classification by hyperspectral satellite imagery," *Proceedings of First Scientific Conference "Earth and Space Sciences for Society"*, Kiev, Ukraine, p. 122, June 2007.

[10] F. Peyrin, R. Goutte, "Image invariant via the Radon transform," *Proceedings of the IEEE International Conference on Image Processing and its Applications*, Maastricht, Netherlands, pp. 458-461, April 1992.

[11] J. Illingworth, J. Kittler, "A survey of the Hough transform," *Computer Vision, Graphics and Image Processing*, vol. 44 (1), pp. 87–116, October 1988.

[12] M. Hussain, D. Chen, A. Cheng, H. Wei, D. Stanley, "Change detection from remotely sensed images: From pixel-based to object-based approaches," *ISPRS Journal of Photogrammetry and Remote Sensing*, vol.80, pp. 91–106, June 2013.

[13] D. Lu, P. Mausel, E. Brondizio, E. Moran, "Change detection techniques," *Int. J. Remote Sensing*, vol. 25, pp. 2365–2407, June 2004.

[14] R. Duca, F. Del Frate, "Hyperspectral and multiangle CHRIS-PROBA images for the generation of land cover maps," *IEEE Transactions on Geoscienceand Remote Sensing*, vol. 46 (10), pp. 2857–2866, October 2008.

[15] S.A. Stankevich, A.A. Kozlova, "Long-term land cover change computer-aided mapping by remote sensed imagery," *Proceedings of the International Conference on Information and Digital Technologies (IDT 2015)*, Žilina, Slovakia, pp. 327–329, July 2014.

[16] J. Zhang, Y. Zeng, W. Xie, T. Wang, "Decision making based on Earth observation technology," In: Deren Li, Jie Shan, Jianya Gong (Eds.), "Geospatial Technology for Earth Observation". Springer, pp. 497–530, September 2009.

Comparison of Methods for Generating Initial Solution for Simulated Annealing

Jaroslav Szabo

***Abstract*—** The article deals with the problem of choosing a method for creating first step solution for metaheuristic method of simulating annealing. Methods are verified on Taillard´s benchmark instances for flow-shop problematic. Three methods are compared based upon their speed, the best created solution and the number of iterations needed to improve result by simulated annealing.

***Keywords*—** flow shop problem, makespan, simulated annealing

I. Introduction

Simulated Annealing (SA) is a metaheuristic method for finding feasible solution. Origin of these methods tracks back to 1980s when Kirkpatrick, Gelatt and Vecchi and independently on them V. Černý described this method in [1] and [2]. Each approach was based on different background but both were tested on Traveling Salesman Problem (TSP). In our article we will discuss how much we can influence the working of SA method, by choosing different method for generating initial solution. Comparison of three different methods which can provide us with initial solution used in SA will be demonstrated on Taillard´s benchmarks for problem of Flow Shop scheduling [3]. We can compare already obtained optimal upper bound solutions with output of our SA method.

II. Simulated Annealing

Metaheuristic methods unlike the heuristic methods allow, under certain conditions, the transition to the solution of inferior value of the objective function, [4]. They consist of the two main parts. The first part is finding the initialisation solution and the calculation of the objective function. The second part is the process of improving the value of objective function in order to search for an optimal solution. We will deal with metaheuristic method of simulated annealing and finding initial solution. In the search for an initial solution we can use many different methods and procedures [5]-[8]. They may include simple heuristic methods or other general practices instead. The diagram below shows a complete scheme of a metaheuristic method. All of the best known metaheuristics have almost the same scheme for evaluating the best possible solution found. We will focus on simulated annealing metaheuristic.

J. Szabo Zilinska Univerzita, Zilina, Slovakia (e-mail: jaroslav.szabo@uniza.sk)

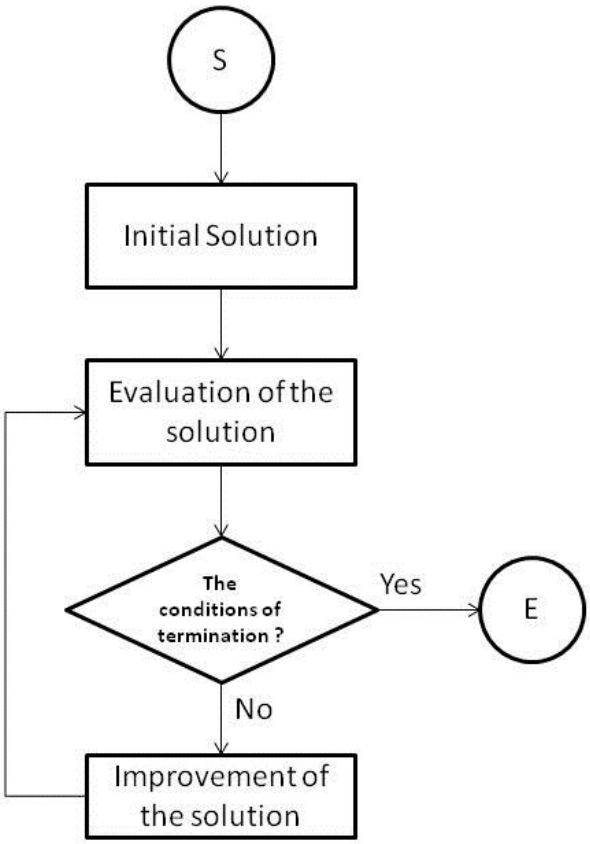

Fig 1 Diagram of metaheuristic

Let us show pseudocode for simulated annealing method.

```
function SA (x, t^max,T^max,β)
  x^best:=x; t:=0;
    T=T^max;
    repeat
        x'=GetRandom(x)
        if AcceptMove(x, x', T) then
            x^best:=KeepBest(x', x^best)
            x:=x';
        end-if
        T=T/(1+βT);
        t:=CPUTime;
    until t > t^max
    return x^best
```

- x^{best} - best found solution
- x - initial solution
- x'- next random solution
- t^{max} - time for method SA to run
- t - elapsed time
- T^{max} - maximum set temperature
- T - current temperature
- β – cooling index

For AcceptMove() method we can choose from several options:

1. The threshold approach when the accept random variable is set on constant value.
2. Monte Carlo approach.
3. Generic approach for bivalent variable.
4. Approach based on temperature. We used this approach for method AcceptMove().

$$p(x',x,T)=\begin{cases} e^{-(f(\mathbf{x}')-f(\mathbf{x}))/T}, & if\ \ f(\mathbf{x}')-f(\mathbf{x})>0; \\ 1 & otherwise. \end{cases}$$

III. LOW SHOP PROBLEMATIC

In general, the scheduling problem consists of positioning resource-demanding activities over time in such a way that the side constrains are respected and an object is minimised. Problems like this arise in diverse areas including production planning, civil engineering, computer science, etc. [9], [10]. In our work we will test effectiveness of initial solution creating methods on flow shop problematic. This is one of NP-hard optimization problems that cannot be solved by exact solving methods in polynomial time. This problem is one of basic scheduling problems of *m* machines and *n* jobs. Every machine *M* can handle only one operation *o* of any job *J* in defined time and only one operation of single job can by handled in defined time [11]. Also, order of operations handled by machines is strictly done so M_1 just does operations o_{i1} to o_{im} and so on. We will test initial methods on problems of 5 machines and 20 jobs, 50 jobs and 100 jobs [3].

IV. METHODS

When we are creating initial solutions for metaheuristic, we can use many different approaches. For example mathematical programming, heuristic methods or other metaheuristic methods. We will focus on three simple methods: Monte Carlo method and operations to rank the elements in the array according to the values of objective function. These methods we will call Weight method 1 and Weight method 2. Weight method 1 will evaluate objective function and rank elements from the best to the worst. Weight method 2 will do the opposite. Our concern will be how fast these methods can work, how good the created solution is compared to the best solution and how many steps are needed to obtain it.

V. RESULTS

All tests will be evaluated on computer Intel Core i7 (2,66GHz), 8GB RAM. First step will be comparison of three tested methods on problem of 5 machines and 20 jobs [3]. All measurement are averaged from 50 repetitions and rounded. In resulting tables we can find these data:

- VOC—Value of objective function created by method.
- VOE—Value of objective function evaluated by SA.
- NOI—Number of iteration of improvement.
- TCI—Time for creating initial solution [ns].

SA parameters were set on time - 250 ms, temperature - 100 and cooling index - 0.01.

Table 1 The results of experiment for 5 machines and 20 jobs

Method	VOC	VOE	NOI	TCI
Monte Carlo	1530	1282	18	4670
Weight method 1	1556	1281	21	24082
Weight method 2	1472	1280	17	17388

Second evaluation tests run on problem of 5 machines and 50 jobs [3].
SA parameters were set on time - 500 ms, temperature - 100 and cooling index - 0.01.

Table 2 The results of experiment for 5 machines and 50 jobs

Method	VOC	VOE	NOI	TCI
Monte Carlo	3198	2727	26	8210
Weight method 1	3119	2727	26	114768
Weight method 2	3240	2727	29	110394

Last set of tests run on problem of 5 machines and 100 jobs [3].
SA parameters were set on time - 1000 ms, temperature - 100 and cooling index - 0.01.

Table 3 The results of experiment for 5 machines and 100 jobs

Method	VOC	VOE	NOI	TCI
Monte Carlo	6198	5494	35	13415
Weight method 1	5981	5495	32	388354
Weight method 2	6258	5494	41	394184

VI. Conclusion

From results obtained in previous section we can draw several conclusions. The best initial values of objective functions of the tested problems were obtained by weighted methods. Monte Carlo is a random method, so obtained values can differ on whole spectrum. Method Monte Carlo is the fastest of the three compared methods. It is a result of the implementation of method Random() in Java programming language. Difference between the numbers of iterations of improvement is not significant enough to determine which method is better. We recommend using the Monte Carlo method which arose between tested methods by incomparable speed and therefore it is useful for creating initial solution for large problems.

References

[1] CERNY, V.: Thermodynamical approach to the traveling salesman problem: An efficient simulation algorithm. Journal of Optimization Theory and Applications, 45, 41-51, 1985.

[2] KIRKPATRICK, S., GERLATT, Jr., C., VECCHI, M.: Optimization by Simulated Annealing. Science 220, 671-680, 1983.

[3] TAILARD, E.: Benchmarks for basic scheduling problems. European Journal of Operational Research 64, 278-285, 1993.

[4] JANACEK, J., HURTIK, J.: An impact of improvement-exchange heuristics to quality of probabilistic TSP. Communications - Scientific Letters of the University of Zilina, 4, 27-35, 2003.

[5] GLOVER, F., KOCHENBERGER, G.: Handbook of metaheuristics 57. Springer, International Series in Operations Research & Management Science, 2003.

[6] CZIMMERMANN, P.: A note on using graphs in regular scheduling problems. Communications - Scientific Letters of the University of Zilina, 4, 47-48, 2003.

[7] BLUM, C., ROLI, A.: Metaheuristics in combinatorial optimization: Overview and conceptual comparison. ACM Computing Surveys, 268-308, 2003.

[8] MARTINCOVA, P.: Performance of simulated grid scheduling algorithms. Journal of Information, Control and Management Systems, Vol. 5, No. 2, 261-270, 2007.

[9] PALUCH, S.: Bus scheduling as a graph coloring problem. Communications - Scientific Letters of the University of Zilina, 4, 16-20, 2003.

[10] JANOSIKOVA, L., HREBEN, M.: Mathematical programming vs. constraint programming for scheduling problems. Communications - Scientific Letters of the University of Zilina, 1, 39-43, 2013.

[11] GAREY, M.R., JOHNSON, D.S., SETHI, R.: The complexity of flowshop and jobshop scheduling. Mathematics of operational research, 1, 117-129, 1976.